A proof of chaos for a seasonally perturbed version of Goodwin growth cycle model: linear and nonlinear formulations

Marina Pireddu [a*]

[a] Dept. of Mathematics and its Applications, University of Milano - Bicocca, U5 Building, Via R. Cozzi 55, 20125 Milano, Italy.

Abstract

We show the existence of complex dynamics for a seasonally perturbed version of Goodwin growth cycle model, both in its original formulation and for a modified formulation, encompassing nonlinear expressions of the real wage bargaining function and of the investment function. The need to deal with a modified formulation of Goodwin model is connected with the economically sensible position of orbits, which have to lie in the unit square, in contrast to what occurs in the model original formulation. In proving the existence of chaos, we follow the seminal idea by Goodwin (1990) of studying forced models in economics. Namely, the original and the modified formulations of Goodwin model are described by Hamiltonian systems, characterized by the presence of a nonisochronous center, and the seasonal variation of the parameter representing the ratio between capital and output, which is common to both frameworks, is empirically grounded. Hence, exploiting the periodic dependence on time of that model parameter we enter the framework of Linked Twist Maps. The topological results valid in this context allow us to prove that the Poincaré map associated with the considered systems is chaotic, focusing on sets that lie in the unit square also when dealing with the original version of Goodwin model. Accordingly, the trademark features of chaos follow, such as sensitive dependence on initial conditions and positive topological entropy.

*E-mail address: marina.pireddu@unimib.it

Keywords: Goodwin growth cycle model, nonisochronous center, parameter seasonal perturbation, linked twist maps, chaotic dynamics.

1 Introduction

In the last years of his research activity, Goodwin in [13] studied, by means of numerical experiments, what can be obtained by the superimposition of exogenous cycles to cycles endogenously generated by a model, focusing in particular on the one by Rössler [33], and concluding that "*At this point it becomes appropriate to consider the relevance, if any, that these forced models have to economics. The answer is not difficult to find: the economy consists of a very large number of separate and distinct parts, with the result that these parts are subject to continual exogenous forces. To begin with there are the individual national economies increasingly acted on by the movements of the world economy. Then within the economy there are various markets with dynamics particular to them. There is the annual solar cycle with its influence on various markets, for example the agricultural, the touristic, the fuel, and any number of others*" [13, pages 121–123].
Taking inspiration from such considerations, we investigate the effect produced on the dynamics of both the original version and a modified formulation of his celebrated growth cycle model (see [11, 12])[1] by the exogenous periodic variation in one of the model parameters, whose seasonal oscillation is empirically grounded.
We recall that the Goodwin model represents, in a "*starkly schematized*" in his own words, yet incisive manner, the involved relationships between capitalists and workers. The need to deal with a modified formulation of the growth cycle model comes from the fact that the original formulation proposed in [11, 12] is not coherent. Indeed, despite the linearity of the real wage bargaining function and of the investment function, the original Goodwin model consists of two nonlinear differential equations of the Lotka-Volterra type, whose variables are wage share in national income and proportion of labor force employed, which by definition cannot exceed unit. On the other hand, orbits of the Goodwin model can lie everywhere in the first

[1] The interested reader can find in [37] a survey on the vast literature about the Goodwin model, concerning possible extensions or modifications of the original setting in [11, 12].

quadrant, possibly outside the unit square.[2] Some contributions, such as those by Desai et al. [8] and Harvie et al. [14] have been devoted to fix such issue in an economic sensible manner. Nonetheless, as shown by Madotto et al. in [18], those works do not solve the problem with the orbit position, since the assumptions made in those two papers are not sufficient to guarantee that orbits lie inside the unit square. Hence, keeping the settings in [8, 14] as starting point, but taking into consideration the results obtained in [18], we here deal with a different reformulation of Goodwin growth cycle model, which in its outcomes is consistent with the meaning of the variables and, in particular, with their admissible range. In more detail, in our model revisitation, in regard to the real wage bargaining function we opt for the nonlinear formulation of the Phillips curve proposed by Phillips in [27], and considered e.g. in [8], while for the investment function we deal with a similar nonlinear formulation, used in the simulative analysis performed in [18] and satisfying the conditions found in that work, so as to ensure that orbits lie in the feasible region. We stress that a nonlinear investment function is grounded also from an economic viewpoint since, according to [9], followed by [39], it is suitable to encompass the description of a more flexible savings behavior with respect to its linear counterpart. Moreover, the nonlinear version of the Phillips curve [27] was initially considered by Goodwin, too, who then linearized that expression in its well-known model so as to obtain an approximation for it "*in the interest of lucidity and ease of analysis*" [11, page 55] (see also [8, page 2666]). Still the economic interpretation requires the real wage bargaining function to be increasing in the proportion of labor force employed, while the investment function has to be decreasing in the wage share in national income.

Since the modified formulation of Goodwin model that we are going to analyze fulfills the conditions in [18], we know that, like the original framework in [11, 12], it is still a Hamiltonian system, characterized by the presence of a global, nonisochronous center. Hence, in order to analytically show what are the dynamic consequences produced on its periodic orbits by the exogenous periodic variation in one of the model parameters, we are going to use the Linked Twist Maps (LTMs hereinafter) method, recently employed for

[2] Goodwin was aware of this fact and indeed in [11, page 57] he wrote "*Both u* [wage share in national income] *and v* [employment proportion] *must be positive and v must, by definition, be less than unity; u normally will be also but may, exceptionally, be greater than unity (wages and consumption greater than total product by virtue of losses and disinvestment)*".

instance in [28] to show the existence of complex dynamics in two evolutionary game theoretic contexts. In particular, we will assume that the chosen parameter alternates in a periodic fashion between two different values, e.g. due to a seasonal effect, and this will allow us to prove the existence of chaotic dynamics. In order to make our choice empirically grounded, we will focus on the parameter that describes the ratio between capital and output, since, keeping the capital level constant, production is no doubt influenced by phenomena that are periodic in nature. We can for instance take into consideration the oscillatory behavior during the solar year of the energy price in electricity markets in consequence of the varying demand over the months, as investigated e.g. in [1, 2], or the different supply in the agricultural commodity markets in the various seasons. We stress however that the same assumption about a periodic variation between two different values made on any other model parameter would produce analogous results in terms of generated dynamics, since all parameters influence the center position.[3]

In order to explain what the LTMs technique consists in we need to recall on the one hand the original setting of linked twist maps, as studied for instance in [5, 31, 32], with the corresponding assumptions of smoothness, preservation of Lebesgue measure and monotonicity of the angular speed with respect to the radial coordinate, and on the other hand the Stretching Along the Paths (henceforth, SAP) method, developed in the planar case in [21, 22] and extended to higher dimensional frameworks in [29]. The SAP method is a topological technique that allows to show the existence of fixed points, periodic points and chaotic dynamics for continuous maps that expand the arcs along one direction and that are defined on sets homeomorphic to the unit cube in Euclidean spaces. The context of LTMs represents a geometrical framework in which it is possible to employ the SAP method in view of proving, as done e.g. in [24, 30], the presence of the trademark features of chaos, such as sensitive dependence on initial conditions and positive topological entropy. In more detail, by a Linked Twist Map we mean the composition of two twist maps, acting each on an annulus, with the two annuli being linked together, i.e., crossing in the two-dimensional case along two (or more) planar

[3]We remark that this is a sufficient, albeit not necessary, condition in order to apply the LTMs method anytime we deal with a nonisochronous center, as long as the switching times between the regimes described by the two different parameter values are large enough. Namely, as shown e.g. in [26, 28], the LTMs technique can be used even when, in consequence of the periodic perturbation of one of the model parameters, the center position does not vary, but the shape of the orbits is modified in a suitable manner.

sets homeomorphic to the unit square, that we call generalized rectangles. Since our approach is purely topological, differently from [5, 31, 32], we just need a twist condition on the boundary of the two linked annuli, similar to what required in the Poincaré-Birkhoff fixed point theorem.
As explained above, in the present paper we are going to apply the LTMs method to the original and to the modified formulations of Goodwin model, that according to the findings in [18] are Hamiltonian systems with a non-isochronous center, whose position varies when changing the value of one of the model parameters. In particular, in both frameworks we will act on the ratio between capital and output, since it is sensible to assume that it alternates, due to a seasonal effect, in a periodic fashion between two different levels, one of which may be seen as a perturbation of the other. In this manner, starting either from the original or the modified formulation of Goodwin model, we obtain two conservative systems, the unperturbed and the perturbed ones, and for each system we can consider an annulus made of energy level lines. Under suitable conditions on the orbits the two annuli are linked together, crossing in two disjoint generalized rectangles. In our settings, the LTMs technique consists in finding two such linked annuli, whose intersections contain chaotic sets: their existence will be established by applying the SAP method to the Poincaré map obtained as composition of the Poincaré maps associated with the unperturbed system and the perturbed one. This leads us to work with discrete-time dynamical systems. Like it happened in other contexts in which the LTMs method was used (see e.g. [28, 30]), also our results about the existence of complex dynamics are robust with respect to small changes, in L^1 norm, in the coefficients of the considered settings.
We stress that the nonisochronicity of the center plays a crucial role in view of applying the SAP method, because it implies that the Poincaré maps produce a twist effect on the linked annuli, since the orbits composing them are run with a different speed. In this manner, the generalized rectangles where the annuli meet are increasingly deformed with the passing of time. Hence, if the regimes governed by the unperturbed system and by the perturbed one are sufficiently long-lasting, the Poincaré maps transform those generalized rectangles into spiral-like sets, that intersect many times the same generalized rectangles, so that the stretching property required by the SAP method in order to guarantee the existence of chaotic sets inside the generalized rectangles is fulfilled.
Regarding the nonisochronicity of the center in the settings that we are going to analyze along the manuscript, for the original formulation proposed

in [11, 12] we can rely on the classical results in [34, 38] about the monotonicity of the period of orbits for the Lotka-Volterra predator-prey model with respect to the energy level, since Goodwin growth cycle model is a special case of that more general framework. For the modified formulation of Goodwin model that we take into account we will instead make reference to the findings obtained in [18] about the period of small and large cycles for a wide class of Hamiltonian systems encompassing the one here considered. More precisely, although an exhaustive analysis of the period of the orbits seems not to be easy to perform, as discussed in [18], due to the presence of singularities in the model, Madotto et al. prove, on the one hand, that the approximation of the period length of small cycles by means of the period of the linearized system is valid near the equilibrium point and, on the other hand, that the period length of large cycles, approaching the boundary of the feasible set, i.e., the unit square in our context, is arbitrarily high. In view of illustrating by means of a concrete example our main result about the existence of complex dynamics for the modified formulation of Goodwin model, we numerically check that the periods of the orbits coinciding with the inner and the outer boundaries of the linked annuli considered in our example do not coincide, finding in particular that the period of the orbits increases with the energy level, in analogy with the classical results in [34, 38] for the original formulation of Goodwin model, and in agreement with the simulative experiments performed in [18] for the same setting that we investigate. Indeed, using a different notation, the framework that we study has been essentially proposed in [18, Subsection 5.3] to illustrate the difficulties which arise when trying to prove that the period map connected with the general class of Hamiltonian systems analyzed in that paper is increasing, even if the detailed numerical simulations performed in [18] suggest that the period monotonicity holds true for the system that we consider.

Hence, our contribution is strongly based, on the one hand, on the results contained in [18] about the period of cycles of a suitable class of Hamiltonian systems. On the other hand, our work belongs to the research strand which, starting from [24, 30], shows how to use the LTMs method to prove the existence of complex dynamics in various continuous-time settings (see e.g. [4, 19, 25]). In more detail, the paper that is closest to ours is [30], where the LTMs method has been applied to investigate the dynamical effects produced by a periodic harvesting in the predator-prey model. Namely, the original formulation of Goodwin growth cycle model is a special case of the Lotka-Volterra predator-prey model. However, our analysis does not coincide with

that performed in [30] since, led by the above explained economic argument about the ratio between capital and output, we will perturb in a periodic fashion a different parameter with respect to [30], and this will produce a dissimilar effect on the center position. Moreover, orbits were run counterclockwise in [30], while they are run clockwise in the present framework, and also this aspect will affect the proof of our result about LTMs, in which we need to count the laps completed by suitable paths around the centers.
In addition to the fact that the LTMs method has not been applied to Goodwin model yet, two further reasons led us to deal in our investigation with its original formulation, too.
The first one is to provide robustness to the results that we shall obtain for the model modified formulation, which indeed in their general conclusions do not depend on the particular expression of the equations involved, as long as we enter the class of Hamiltonian systems considered in [18]. Only the kind of geometrical configuration for orbits in the phase plane, and thus the way to use the LTMs method, could vary according to the formulation of the model equations and on the basis of how they depend on the parameter that is periodically perturbed. We remark that different nonlinear expressions for the real wage bargaining function and for the investment function could be sensible, as well. Nonetheless, we chose two formulations that, in addition to have been already considered in the existing literature, satisfy the conditions found in [18] ensuring that the center is nonisochronous and that orbits lie in the feasible region, i.e., the unit square, since the state variables, being wage share in national income and proportion of labor force employed, can neither be negative, nor exceed unity.
The second reason for considering Goodwin original formulation of the growth cycle model lies in the possibility of showing how to use the LTMs method to prove the existence of chaotic sets lying inside the unit square, despite the previously mentioned issue with the orbit position in the original Goodwin setting. Namely, the chaotic sets are contained in the detected pair of linked annuli, that jointly constitute an invariant set under the action of the Poincaré map obtained as composition of the Poincaré maps associated with the unperturbed system and the perturbed one, since each annulus, being made of periodic orbits, is invariant under the action of the Poincaré map describing the corresponding regime. Choosing then linked together annuli contained in the unit square solves the problem. As our illustrative examples will show, this can be done even when dealing with parameter configurations analogous to those considered in [8, 14]. We stress that the issue with the

orbit position did not occur in [30], since the variables in the original Lotka-Volterra model, describing the size of the prey and the predator populations, are not confined to lie in the unit square.
The remainder of the paper is organized as follows. In Section 2 we recall the original formulation of Goodwin growth cycle model and we explain how to apply the LTMs method to such context, highlighting the differences with [30]. In Section 3 we introduce the modified formulation of Goodwin model, for which we check the existence of chaotic dynamics via the LTMs technique. In Section 4 we recall the definitions and the results connected with the LTMs method that have been used in the preceding sections. In Section 5 we conclude. The Appendix contains the mathematical proof of our results, as well as some related comments.

2 The LTMs method for Goodwin model original formulation

Following Goodwin seminal idea in [13] of studying forced models in economics, we are going to apply the Linked Twist Maps (henceforth, LTMs) method, whose main features are described in Section 4, to his celebrated growth cycle model, in order to show the effects produced on its dynamics by the exogenous periodic variation in one of the model parameters, whose seasonal oscillation is empirically grounded.
We start by briefly recalling the model original formulation proposed in [11, 12].
Denoting by $u(t) \in [0,1]$ the wage share in national income and by $v(t) \in [0,1]$ the employment proportion, Goodwin model reads as

$$\begin{cases} u' = u\left(-(\alpha+\chi)+\rho v\right) \\ v' = v\left(-(\alpha+\beta)+\frac{1-u}{\sigma}\right) \end{cases} \tag{2.1}$$

where all parameters are positive and, in particular, α is the exogenous labor productivity growth rate, β is the exogenous labor force growth rate, σ is the capital-output ratio, while χ and ρ characterize[4] the real wage growth rate, which is of the form $-\chi+\rho v$. The first equation in (2.1) derives from

[4]We stress that, rather than χ, the symbol γ is generally used in the Goodwin model. However, we prefer to save γ to denote paths (see e.g. Definition 4.1) in agreement with the existing literature on the SAP method.

the Goodwin's linearized version of the Phillips curve [27] in real wages (see the first equation in (3.1) for its nonlinear formulation), while we refer the interested reader to [8] for the derivation of the second equation, based on the assumptions that capitalists reinvest all profits and workers consume all wages, and to [8, 14] for further details on the model.
Although state variables, due to their meaning, can neither be negative nor exceed unity, the latter condition is not guaranteed by (2.1). Namely, those equations describe a conservative system with closed orbits lying everywhere in the first quadrant of $\mathbb{R}^2$ and surrounding the center

$$P = \left(1 - \sigma(\alpha + \beta)\,, \frac{\alpha + \chi}{\rho}\right).$$

We stress that P lies in the unit square when

$$\sigma < \frac{1}{\alpha + \beta}\,, \qquad \alpha + \chi < \rho\,. \tag{2.2}$$

Also the origin $O = (0, 0)$ is an equilibrium, being a saddle. As it is immediate to check, System (2.1) is a special case of the Lotka-Volterra predator-prey model (see e.g. [3])

$$\begin{cases} x' = x\,(a - by) \\ y' = y\,(-c + dx) \end{cases} \tag{2.3}$$

where $u(t)$ corresponds to $y(t)$ and $v(t)$ corresponds to $x(t)$, even if $x(t)$ and $y(t)$ are not confined to lie in $[0, 1]$, since they are non-negative variables describing the size of the prey and of the predator populations, respectively. In particular, like in [30] we focused just on $x(t) > 0$ and $y(t) > 0$, being therein interested in dynamic outcomes characterized by the coexistence between preys and predators, in what follows we will confine our analysis to positive values of $u(t)$ and $v(t)$. Namely, System (2.3) describes the twofold, at one time beneficial and detrimental, nature of the interactions between predators and preys. Similarly, the Goodwin model schematically represents the involved relationship between capitalists and workers, with the wage share in national income being the predator variable and the employment proportion being the prey.
Both (2.1) and (2.3) describe Hamiltonian systems. In the former case, orbit equations are given by

$$E(u, v) = \frac{u}{\sigma} - \left(\frac{1}{\sigma} - \alpha - \beta\right)\log(u) + \rho v - (\alpha + \chi)\log(v) = \ell,$$

for some $\ell \geq \ell_0$, where ℓ_0 is the minimum energy level attained by $E(u, v)$ on the open unit square $(0, 1)^2$, i.e., $\ell_0 = E(P)$. Notice that, under (2.2), the minimum level attained by $E(u, v)$ on $(0, 1)^2$ coincides with the minimum level attained on $(0, +\infty)^2$, since we are assuming that $P \in (0, 1)^2$. Moreover, the period of the orbits of System (2.1) is increasing with the energy level, due to the possibility of relying on the classical results in [34, 38] on the monotonicity of the period of the orbits for the Lotka-Volterra predator-prey model in (2.3). On the other hand, contrary to what happens with System (2.3), orbits for System (2.1) are run clockwise, as the analysis of the phase portrait shows. This is due to the fact that, as observed above, comparing Systems (2.1) and (2.3) we have that $u(t)$ corresponds to $y(t)$ and $v(t)$ corresponds to $x(t)$.

While Goodwin investigated by means of numerical experiments in [13] the dynamic outcomes that can be obtained superimposing exogenous cycles to cycles endogenously generated by a model, we will analytically show the effect produced on the periodic orbits of System (2.1) by the exogenous periodic variation in one of the model parameters. In view of making our choice empirically grounded, we will focus on σ, i.e., the capital-output ratio, since, keeping the capital level constant, production is certainly influenced by phenomena that are periodic in nature. We can e.g. consider the oscillatory behavior during the solar year of the energy price in electricity markets in consequence of the varying demand over the months or the different supply in the agricultural commodity markets in the various seasons. To fix ideas, we concentrate on the second phenomenon, since it is clear that north of the equator, for instance in Europe and in the United States, supply in the agricultural commodity markets is larger from April to October than during the remaining part of the year. Hence, for the capital-output ratio σ we can assume a periodic alternation between a higher value, that we will call $\sigma^{(I)}$, referring to fall and winter, and a lower value, which may be seen as a perturbation of the former, that we will call $\sigma^{(II)}$, referring to spring and summer.[5] We stress however that a similar assumption about a periodic variation made on any other model parameter would produce analogous results in terms of generated dynamics, since all parameters affect, in some way, the center position.

[5]In regard to seasonal variations in demand and energy price in electricity markets, according to [2], which refers to [1], "*Cycles and seasonality have for a long time been observed in electricity markets. There are hourly, daily, weekly, and seasonal fluctuations in prices and demand*". See also [17] for a seasonal electricity demand and pricing analysis.

Supposing then that the capital-output ratio alternates between $\sigma^{(I)}$, for $t \in [0, T^{(I)})$, and $\sigma^{(II)}$, for $t \in [T^{(I)}, T^{(I)} + T^{(II)})$, with $\sigma^{(I)} > \sigma^{(II)}$, and that the same alternation between the two regimes recurs with T-periodicity, where $T = T^{(I)} + T^{(II)}$, we can assume that we are dealing with a system with periodic coefficients of the form

$$\begin{cases} u' = u\left(-(\alpha(t) + \chi(t)) + \rho(t)v\right) \\ v' = v\left(-(\alpha(t) + \beta(t)) + \frac{1-u}{\sigma(t)}\right) \end{cases} \tag{2.4}$$

where

$$k(t) \equiv k, \text{ for } k \in \{\alpha, \beta, \chi, \rho\}, \text{ and } \sigma(t) = \begin{cases} \sigma^{(I)} & \text{for } t \in [0, T^{(I)}) \\ \sigma^{(II)} & \text{for } t \in [T^{(I)}, T) \end{cases} \tag{2.5}$$

with

$$0 < \sigma^{(II)} < \sigma^{(I)} < \frac{1}{\alpha + \beta}, \qquad \alpha + \chi < \rho \tag{2.6}$$

as a consequence of (2.2). The function $\sigma(t)$ is supposed to be extended to the whole real line by T-periodicity.
When the capital-output ratio takes value $\sigma^{(i)}$, and thus we are in the regime whose dynamics are governed by the system that we will call (i), the center coincides with $P^{(i)} = \left(1 - \sigma^{(i)}(\alpha + \beta), \frac{\alpha+\chi}{\rho}\right)$, for $i \in \{I, II\}$. Notice that, passing from $P^{(I)}$ to $P^{(II)}$, the ordinate of the center does not change, while its abscissa raises. As concerns orbits, they are closed for both Systems (I) and (II), surrounding $P^{(I)}$ and $P^{(II)}$, respectively, and they are run clockwise. In the former case, orbits have equation

$$E^{(I)}(u, v) = \frac{u}{\sigma^{(I)}} - \left(\frac{1}{\sigma^{(I)}} - \alpha - \beta\right)\log(u) + \rho v - (\alpha + \chi)\log(v) = \ell, \tag{2.7}$$

for some $\ell \geq \ell_0^{(I)}$, while, in the latter case, orbits have equation

$$E^{(II)}(u, v) = \frac{u}{\sigma^{(II)}} - \left(\frac{1}{\sigma^{(II)}} - \alpha - \beta\right)\log(u) + \rho v - (\alpha + \chi)\log(v) = h, \tag{2.8}$$

for some $h \geq h_0^{(II)}$, where $\ell_0^{(I)}$ and $h_0^{(II)}$ are the minimum energy levels attained by $E^{(I)}(u, v)$ and $E^{(II)}(u, v)$ on $(0, 1)^2$, respectively, i.e., $\ell_0^{(I)} =$

$E^{(I)}(P^{(I)})$ and $h_0^{(II)} = E^{(II)}(P^{(II)})$.
The sets $\Gamma^{(I)}(\ell) = \{(u,v) \in (0,+\infty)^2 : E^{(I)}(u,v) = \ell\}$, for $\ell > \ell_0^{(I)}$, are simple closed curves surrounding $P^{(I)}$, while $\Gamma^{(II)}(h) = \{(u,v) \in (0,+\infty)^2 : E^{(II)}(u,v) = h\}$, for $h > h_0^{(II)}$, are simple closed curves surrounding $P^{(II)}$. We call *annulus around $P^{(I)}$ for System (I)* any set $\mathcal{C}^{(I)}(\ell_1,\ell_2) = \{(u,v) \in (0,+\infty)^2 : \ell_1 \leq E^{(I)}(u,v) \leq \ell_2\}$ with $\ell_0^{(I)} < \ell_1 < \ell_2$, whose inner boundary coincides with $\Gamma^{(I)}(\ell_1)$ and whose outer boundary coincides with $\Gamma^{(I)}(\ell_2)$. Similarly, we call *annulus around $P^{(II)}$ for System (II)* any set $\mathcal{C}^{(II)}(h_1,h_2) = \{(u,v) \in (0,+\infty)^2 : h_1 \leq E^{(II)}(u,v) \leq h_2\}$ with $h_0^{(II)} < h_1 < h_2$, whose inner boundary coincides with $\Gamma^{(II)}(h_1)$ and whose outer boundary coincides with $\Gamma^{(II)}(h_2)$. In particular, we are interested in annuli for Systems (I) and (II) contained in $(0,1)^2$, due to the meaning of variables u and v. This configuration will be achieved by choosing annuli whose outer (and consequently, inner) boundary set lies sufficiently close to the corresponding center, i.e., for low enough values of the energy levels $\ell_2 > \ell_0^{(I)}$ and $h_2 > h_0^{(II)}$ (see e.g. Figure 1).
In view of providing conditions on the energy levels that ensure that two annuli are linked together, thus crossing in two disjoint generalized rectangles (see Section 4 for the corresponding definition), let us consider on the straight line r joining $P^{(I)}$ and $P^{(II)}$, having equation $v = (\alpha+\chi)/\rho$, the ordering inherited from the horizontal axis, so that given the points $R = (u_R, v^*)$ and $S = (u_S, v^*)$ belonging to r, hence with $v^* = (\alpha+\chi)/\rho$, it holds that $R \lhd S$ (resp. $R \trianglelefteq S$) if and only if $u_R < u_S$ (resp. $u_R \leq u_S$). We are now in position to introduce the following:

Definition 2.1 *Given the annulus $\mathcal{C}^{(I)}(\ell_1,\ell_2)$ around $P^{(I)}$ and the annulus $\mathcal{C}^{(II)}(h_1,h_2)$ around $P^{(II)}$, we say that they are linked together if*

$$P_{2,-}^{(I)} \lhd P_{1,-}^{(I)} \trianglelefteq P_{2,-}^{(II)} \lhd P_{1,-}^{(II)} \trianglelefteq P_{1,+}^{(I)} \lhd P_{2,+}^{(I)} \trianglelefteq P_{1,+}^{(II)} \lhd P_{2,+}^{(II)}$$

where, for $j \in \{1,2\}$, $P_{j,-}^{(I)}$ and $P_{j,+}^{(I)}$ denote the intersection points between $\Gamma^{(I)}(\ell_j)$ and the straight line r, with $P_{j,-}^{(I)} \lhd P^{(I)} \lhd P_{j,+}^{(I)}$, and, similarly, $P_{j,-}^{(II)}$ and $P_{j,+}^{(II)}$ denote the intersection points between $\Gamma^{(II)}(h_j)$ and r, with $P_{j,-}^{(II)} \lhd P^{(II)} \lhd P_{j,+}^{(II)}$.

We stress that, for $\ell_j > \ell_0^{(I)}$ and $h_j > h_0^{(II)}$, $j \in \{1,2\}$, the boundary sets $\Gamma^{(I)}(\ell_j)$ and $\Gamma^{(II)}(h_j)$ intersect the straight line r in exactly two points because

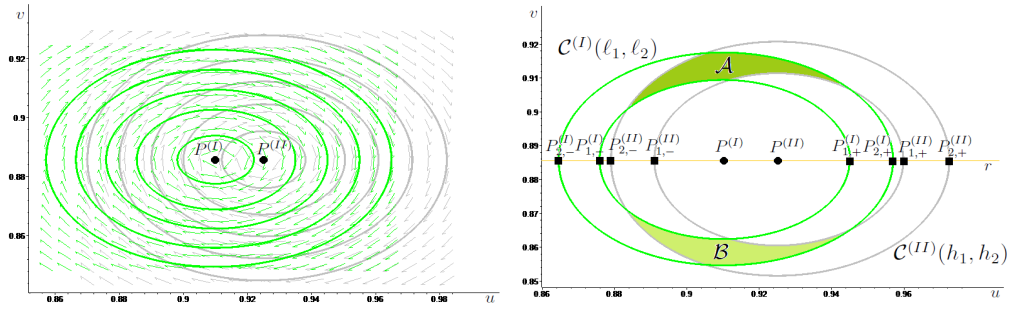

(A) (B)

Figure 1: In (A) we draw in green some energy level lines associated with System (I), surrounding $P^{(I)}$, and in gray some energy level lines associated with System (II), surrounding $P^{(II)}$, together with the corresponding phase portrait. In (B), we illustrate Definition 2.1, showing how to obtain two linked together annuli by suitably choosing two level lines for each system. In particular, we call $\mathcal{C}^{(I)}(\ell_1,\ell_2)$, $\mathcal{C}^{(II)}(h_1,h_2)$ the two linked annuli, and $\mathcal{A}$ (colored in dark green), $\mathcal{B}$ (colored in light green) the two disjoint generalized rectangles obtained as intersection between the two annuli.

$\{(u,v)\in(0,+\infty)^2 : E^{(I)}(u,v)\le\ell\}$ and $\{(u,v)\in(0,+\infty)^2 : E^{(II)}(u,v)\le h\}$, coinciding with the lower contour sets of the convex functions $E^{(I)}$ in (2.7) and $E^{(II)}$ in (2.8), are star-shaped for all $\ell>\ell_0^{(I)}$ and for every $h>h_0^{(II)}$, respectively. We refer the reader to Figure 1 (B) for a graphical illustration of Definition 2.1.

We recall that a geometrical configuration analogous to that depicted in Figure 1 (B), except for the need for orbits to lie in the unit square, was found in [25] (cf. Figure 2 therein), where the LTMs method was applied to a periodically forced asymmetric second order ODE. However in that case the abscissa of the center decreased passing from the unperturbed regime to the perturbed one and the centers of the systems corresponding to the two regimes were located on the horizontal axis. Although both dissimilarities would not require to introduce relevant differences in the statement and proof of the main result in [25] (cf. Theorem 1.2 therein), in adapting them to our framework we will provide a slightly more general[6] version of [25, Theorem

[6]In [25, Theorem 1.2] the special case of Proposition 2.1 with $m^{(I)}=m\ge 2$ and $m^{(II)}=1$ was considered.

1.2] in Proposition 2.1, together with a complete proof (contained in the Appendix) for the reader's convenience.
To such aim, in addition to exploiting the tools recalled in Section 4 and in particular the stretching relation in (4.1), we need to introduce the Poincaré map Ψ of System (2.4), which associates with any initial condition (u_0, v_0) belonging to $(0, +\infty)^2$ the position at time T of the solution $\varsigma(\,\cdot\,, (u_0, v_0)) = (u(\,\cdot\,, (u_0, v_0)), v(\,\cdot\,, (u_0, v_0)))$ to (2.4) starting at time $t = 0$ from (u_0, v_0). In symbols, $\Psi : (0, +\infty)^2 \to (0, +\infty)^2$, $(u_0, v_0) \mapsto \varsigma(T, (u_0, v_0))$. Along the paper solutions are meant in the Carathéodory sense, being absolutely continuous and satisfying the corresponding system for almost every $t \in \mathbb{R}$. We recall that a classical method to show the existence of periodic solutions for systems of first order ODEs with periodic coefficients is based on the search of the periodic points for the associated Poincaré map, under the assumption of uniqueness of the solutions for the Cauchy problems (cf. [16]). Notice that Ψ is a homeomorphism on $(0, +\infty)^2$ and that it may be decomposed as $\Psi = \Psi^{(II)} \circ \Psi^{(I)}$, where $\Psi^{(I)}$ is the Poincaré map associated with System (I) for $t \in [0, T^{(I)}]$ and $\Psi^{(II)}$ is the Poincaré map associated with System (II) for $t \in [0, T^{(II)}]$. Moreover, since every annulus $\mathcal{C}^{(I)}(\ell_1, \ell_2)$ around $P^{(I)}$ is invariant under the action of the map $\Psi^{(I)}$, being composed of the invariant orbits $\Gamma^{(I)}(\ell)$, for $\ell \in [\ell_1, \ell_2]$, and, similarly, since every annulus $\mathcal{C}^{(II)}(h_1, h_2)$ around $P^{(II)}$ is invariant under the action of the map $\Psi^{(II)}$, it holds that every pair of linked together annuli is invariant under the action of the composite map Ψ. In Proposition 2.1 we will denote by $\tau^{(I)}(\ell)$, for all $\ell > \ell_0^{(I)}$, the period of $\Gamma^{(I)}(\ell)$, i.e., the time needed by the solution $\varsigma^{(I)}(\,\cdot\,, (u_0, v_0))$ to System (I), starting from any $(u_0, v_0) \in \Gamma^{(I)}(\ell)$, to complete one turn around $P^{(I)}$ moving along $\Gamma^{(I)}(\ell)$, and by $\tau^{(II)}(h)$, for all $h > h_0^{(II)}$, the period of $\Gamma^{(II)}(h)$, i.e., the time needed by the solution $\varsigma^{(II)}(\,\cdot\,, (u_0, v_0))$ to System (II), starting from any $(u_0, v_0) \in \Gamma^{(II)}(h)$, to complete one turn around $P^{(II)}$ moving along $\Gamma^{(II)}(h)$. Orbits surrounding either $P^{(I)}$ or $P^{(II)}$ are run clockwise and $\tau^{(I)}(\,\cdot\,)$ and $\tau^{(II)}(\,\cdot\,)$ are monotonically increasing with the energy levels, since both features are fulfilled for System (2.1), as remarked above. Hence, for any annulus $\mathcal{C}^{(I)}(\ell_1, \ell_2)$ around $P^{(I)}$ it holds that $\tau^{(I)}(\ell_1) < \tau^{(I)}(\ell_2)$, as well as for each annulus $\mathcal{C}^{(II)}(h_1, h_2)$ around $P^{(II)}$ it holds that $\tau^{(II)}(h_1) < \tau^{(II)}(h_2)$.
Our result about System (2.4) reads as follows:

Proposition 2.1 *For any choice of the positive parameters α, β, χ, $\rho, \sigma^{(I)}$, $\sigma^{(II)}$ satisfying (2.6), given the annulus $\mathcal{C}^{(I)}(\ell_1, \ell_2)$ around $P^{(I)}$, for some $\ell_0^{(I)} < \ell_1 < \ell_2$, and the annulus $\mathcal{C}^{(II)}(h_1, h_2)$ around $P^{(II)}$, for some $h_0^{(II)} <$*

$h_1 < h_2$, assume that they are linked together, calling $\mathcal{A}$ and $\mathcal{B}$ the connected components of $\mathcal{C}^{(I)}(\ell_1, \ell_2) \cap \mathcal{C}^{(II)}(h_1, h_2)$. Then, for every $m^{(I)} \geq 1$ and $m^{(II)} \geq 1$ with $m = m^{(I)} m^{(II)} \geq 2$ there exist two positive constants $t^{(I)} = t^{(I)}(m^{(I)}, \tau^{(I)}(\ell_1), \tau^{(I)}(\ell_2))$ and $t^{(II)} = t^{(II)}(m^{(II)}, \tau^{(II)}(h_1), \tau^{(II)}(h_2))$ such that if $T^{(i)} > t^{(i)}$, for $i \in \{I, II\}$, the Poincaré map $\Psi = \Psi^{(II)} \circ \Psi^{(I)}$ of System (2.4) induces chaotic dynamics on m symbols in $\mathcal{A}$ and in $\mathcal{B}$, and all the properties listed in Theorem 4.1 are fulfilled for Ψ.

According to Proposition 2.1, whenever we have two linked together annuli related to Systems (I) and (II), if the switching times between the regimes described by those two systems are large enough, then the Poincaré map $\Psi = \Psi^{(II)} \circ \Psi^{(I)}$ induces chaotic dynamics on $m \geq 2$ symbols in the sets in which the two annuli intersect. As it is clear from the proof of Proposition 2.1 (see the Appendix), that chaotic behavior is generated by the twist effect produced on the linked annuli by the different speeds with which their inner and outer boundary sets are run. Namely, after a long enough time, this twist effect suffices to make the image through $\Psi^{(I)}$ and $\Psi^{(II)}$ of the paths joining the inner and the outer boundary sets of the annuli spiral inside them and cross many times the intersection sets $\mathcal{A}$ and $\mathcal{B}$ between the linked annuli. In this manner, Ψ satisfies the stretching relation described in Theorem 4.1 and thus all properties listed therein hold true for the composite Poincaré map.

We further notice that, under the assumptions in (2.6), which ensure that the centers of Systems (I) and (II) belong to the open unit square, when applying Proposition 2.1 to linked annuli whose inner and outer boundary sets lie sufficiently close to those centers, i.e., for low enough values of the energy levels $\ell_2 > \ell_1 > \ell_0^{(I)}$ and $h_2 > h_1 > h_0^{(II)}$, the chaotic invariant sets contained in $\mathcal{A}$ and in $\mathcal{B}$ lie in the open unit square, too. The same is true not only for the chaotic sets, but for a whole pair of linked annuli when the outer boundary sets $\Gamma^{(I)}(\ell_2)$ and $\Gamma^{(II)}(h_2)$ are contained in $(0,1)^2$, like it happens for instance in Figure 1 (A), where we fix[7] $\alpha = 0.02$, $\beta = 0.01$, $\chi = 0.6$, $\rho = 0.7$, $\sigma^{(I)} = 3$, $\sigma^{(II)} = 2.5$, so that $P^{(I)} = (0.910, 0.886)$ and $P^{(II)} = (0.925, 0.886)$. In particular, as shown in Figure 1 (B), we obtain two linked together annuli $\mathcal{C}^{(I)}(\ell_1, \ell_2)$ and $\mathcal{C}^{(II)}(h_1, h_2)$, contained in $(0,1)^2$

[7]We stress that such parameter configuration is analogous to that considered in [14, page 77], where the parameter values are $\alpha = 0.03$, $\beta = 0.01$, $\chi = 0.63$, $\rho = 0.7$, $\sigma = 3$, and similar to the one in [8, page 2668], where the authors set $\alpha = 0.001$, $\beta = 0.001$, $\chi = 0.95$, $\rho = 1$, $\sigma = 3$, recalling that in those works the symbol γ was used instead of χ.

and crossing in the two disjoint generalized rectangles denoted by $\mathcal{A}$ and $\mathcal{B}$, e.g. for $\ell_1 = 1.0274$, $\ell_2 = 1.0276$, $h_1 = 1.0943$, $h_2 = 1.0946$.
Indeed, despite the previously recalled issue (see (2.2) and the lines above it) with the orbit position for the original formulation of the Goodwin model in (2.1), every annulus around $P^{(i)}$ for System (i), with $i \in \{I, II\}$, being made of periodic orbits, is invariant under the action of the Poincaré map $\Psi^{(i)}$. Consequently, each pair of linked annuli jointly constitutes an invariant set under the action of the composite Poincaré map $\Psi = \Psi^{(II)} \circ \Psi^{(I)}$, so that, even for System (2.1), the LTMs method allows to detect complex dynamics that are consistent from an economic viewpoint.
Nonetheless, in Section 3 we will introduce and analyze a modified formulation of Goodwin growth cycle model (cf. (3.1)), whose orbits are all contained in the unit square, since the necessary and sufficient conditions found in [18] are fulfilled.
Before turning to that new framework we stress that, like [25, Theorem 1.2], also Proposition 2.1 is robust with respect to small changes, in L^1 norm, in the coefficients of System (2.4). Namely, from the proof of Proposition 2.1 it follows that if $T^{(I)}$ and $T^{(II)}$ satisfy the conditions described in its statement, then, recalling System (2.4) and the definition of its coefficients in (2.5), there exists a positive constant ε such that the same conclusions of Proposition 2.1 hold true for the system

$$\begin{cases} u' = u\left(-(\breve{\alpha}(t) + \breve{\chi}(t)) + \breve{\rho}(t)v\right) \\ v' = v\left(-(\breve{\alpha}(t) + \breve{\beta}(t)) + \frac{1-u}{\breve{\sigma}(t)}\right) \end{cases}$$

with $\breve{\alpha}$, $\breve{\beta}$, $\breve{\chi}$, $\breve{\rho}$, $\breve{\sigma} : \mathbb{R} \to \mathbb{R}$ being T-periodic functions with $T = T^{(I)} + T^{(II)}$, as long as

$$\int_0^T \left| \breve{k}(t) - k \right| dt < \varepsilon, \quad \text{for } k \in \{\alpha, \beta, \chi, \rho\},$$

and

$$\int_0^T \left| \breve{\sigma}(t) - \sigma(t) \right| dt = \int_0^{T^{(I)}} \left| \breve{\sigma}(t) - \sigma^{(I)} \right| dt + \int_{T^{(I)}}^T \left| \breve{\sigma}(t) - \sigma^{(II)} \right| dt < \varepsilon.$$

Due to the similar arguments that are needed in its proof, also Proposition 3.1, i.e. the main result that we shall present in Section 3 about the Goodwin model modified formulation, is robust with respect to small changes in the coefficients of System (3.5), in L^1 norm.

We conclude the present section by recalling that in [30] the LTMs method has been applied to the Lotka-Volterra System (2.3) under the assumption of a periodic harvesting, that perturbed the center position, causing an alternation for it between two points. However, since in [30] it was supposed that not only preys, but also predators decrease in number during the harvesting season, then both coordinates of the center change in that framework. Furthermore, orbits of System (2.3) are run counterclockwise, rather than clockwise like it happens with the orbits of System (2.1), and thus the definition of the rotation number used in [30] does not coincide with that employed in the proof of Proposition 2.1 (cf. (6.3) and (6.4)). Those two differences between [30] and the above described context pushed us to provide a specific, complete presentation in the here analyzed setting of the LTMs method and of its application to (2.1) in Proposition 2.1. Indeed, as recently shown in [28], the way in which the LTMs method can be used depends on the meaning attached to the variables and parameters of the considered model. Moreover, the detailed presentation of the LTMs method provided above is useful in view of Section 3, too, where it will suffice for us to focus on the main steps, highlighting the dissimilarities with what we have already explained.

3 The Goodwin model modified formulation

Rather than dealing with the linear expressions for the real wage bargaining function and for the investment function seen in Section 2, we now consider a modified formulation of such setting, motivated by the issue with the orbit position in the original Goodwin model [11].
As concerns the real wage bargaining function, the most natural choice is given by the Phillips nonlinear specification in [27], even if for real rather than money wages (cf. the first equation in System (3.1)). This was indeed what Goodwin initially assumed, before linearizing the Phillips curve so as to obtain the first equation in (2.1) as an approximation (see [11, page 55]). We recall that the nonlinear formulation of the Phillips curve in [27] has been considered e.g. by Desai et al. in [8], too, in their attempt to guarantee that the orbits of the growth cycle model lie inside the unit square. On the other hand, as shown by Madotto et al. in [18], the attempt by Desai et al. in [8] is not successful in fixing the problem with the orbit position because of their choice of the investment function (cf. equation (10) in [8, page 2667]), that describes a framework in which capitalists, depending on profitability,

do not necessarily invest all profits. We stress that in [18] it is proven that even the modified version of the Goodwin model proposed by Harvie et al. in [14] does not ensure that orbits lie inside the unit square. In order to avoid similar issues, for the investment function we consider a nonlinear formulation (see the second equation in System (3.1)) satisfying the conditions found in [18] and that we shall recall below, so as to guarantee that orbits lie in the feasible region. In more detail, for the investment function we deal with the formulation used in the simulative analysis performed in [18, Subsection 5.3]. We underline that a nonlinear investment function is grounded also from an economic viewpoint since, according to [9], followed by [39], it is suitable to describe a more flexible savings behavior. Still the economic interpretation requires the real wage bargaining function to be increasing in the proportion of labor force employed, while the investment function has to be decreasing in the wage share in national income.
Since the modified formulation of the Goodwin model in (3.1) that we are going to analyze satisfies the conditions in [18], we know that, like the original framework in [11, 12], it is still a Hamiltonian system characterized by the presence of a global, nonisochronous center. Hence, in order to analytically show what are the dynamic consequences produced on its periodic orbits by an exogenous periodic variation in one of the model parameters, we are going to use the LTMs method. In particular, in view of making our parameter choice empirically grounded, due to the same argument explained in Section 2 we will focus on the parameter that describes the ratio between capital and output, assuming that it alternates in a periodic fashion between two different values, e.g. due to a seasonal effect. This will allow us to prove the existence of chaotic dynamics for System (3.5), i.e. the analogue of System (2.4) obtained from (3.1). Nonetheless, as explained in Section 2, assuming a periodic variation on any other model parameter would lead to analogous conclusions about the system dynamic behavior, since the center position is influenced by all parameters.
In symbols, still denoting by $u(t) \in [0,1]$ the wage share in national income and by $v(t) \in [0,1]$ the employment proportion, our modified formulation of the Goodwin model reads as

$$\begin{cases} u' = u\left(-(\chi+\alpha) + \frac{\rho}{(1-v)^{\delta}}\right) \\ v' = v\left(-(\alpha+\beta) + \frac{1}{\sigma}\left(c - \frac{\eta}{(1-u)^{\mu}}\right)\right) \end{cases} \tag{3.1}$$

where all parameters are positive and, in addition to α, β and σ, that still describe the exogenous labor productivity growth rate, the exogenous labor force growth rate and the capital-output ratio, respectively, we have that χ, ρ and δ characterize the real wage growth rate, which, in agreement with [27], is now of the form $-\chi+\frac{\rho}{(1-v)^\delta}$, while c, η and μ, together with σ, characterize the output growth rate, now formulated as $\frac{1}{\sigma}\left(c-\frac{\eta}{(1-u)^\mu}\right)$. In particular, as in the model original version in [11, 12], it is assumed that capitalists reinvest all profits and workers consume all wages.
In addition to the origin $O=(0,0)$, which is still a saddle, the other equilibrium for System (3.1) is given by

$$\widehat{P}=\left(1-\left(\frac{\eta}{c-\sigma(\alpha+\beta)}\right)^{\frac{1}{\mu}},\,1-\left(\frac{\rho}{\chi+\alpha}\right)^{\frac{1}{\delta}}\right),$$

that belongs to the open unit square $(0,1)^2$ when

$$\sigma<\frac{c-\eta}{\alpha+\beta}\,,\quad \rho<\chi+\alpha\,,\quad \delta\geq 1,\quad \mu\geq 1. \tag{3.2}$$

In order to ensure that $\widehat{P}$ is a global center for System (3.1), whose orbits lie in the square $(0,1)^2$, which is again the feasible region due to the meaning of u and v, and in view of applying some results obtained in [18] on the period of orbits, we need to check that the conditions described on page 778 therein for the general system

$$\begin{cases} u'=u\,f(u)\,\psi(v)\\ v'=-v\,g(v)\,\varphi(u)\end{cases} \tag{3.3}$$

are fulfilled with the considered formulations of the real wage bargaining function and of the investment function, under the parameter assumptions in (3.2). When adapted to our framework, the conditions in [18] require that f, $g:(0,1)\to(0,+\infty)$ are continuous functions and that φ, $\psi:(0,1)\to\mathbb{R}$ are $\mathcal{C}^1$ maps with positive derivative on $(0,1)$, satisfying $\lim_{u\to 0^+}\varphi(u)\in(-\infty,0)$, $\lim_{v\to 0^+}\psi(v)\in(-\infty,0)$, $\lim_{u\to 1^-}\varphi(u)>0$, $\lim_{v\to 1^-}\psi(v)>0$. All this is true in our context since, setting $f(u)=1$, $\psi(v)=-(\chi+\alpha)+\frac{\rho}{(1-v)^\delta}$, $g(v)=1$, $\varphi(u)=(\alpha+\beta)-\frac{1}{\sigma}\left(c-\frac{\eta}{(1-u)^\mu}\right)$, it holds that f, g are continuous maps taking positive values only and φ, ψ are $\mathcal{C}^1$ increasing maps

on $(0,1)$, satisfying

$$\begin{aligned}
&\lim_{u\to 0^+}\varphi(u)=\alpha+\beta-\tfrac{1}{\sigma}\,(c-\eta)\in(-\infty,0),\\
&\lim_{v\to 0^+}\psi(v)=-(\chi+\alpha)+\rho\in(-\infty,0),\\
&\lim_{u\to 1^-}\varphi(u)=+\infty,\quad \lim_{v\to 1^-}\psi(v)=+\infty
\end{aligned}$$

under (3.2). Moreover, setting

$$A(u)=\int\frac{\varphi(u)}{uf(u)}\,du=\int\frac{1}{u}\left((\alpha+\beta)-\frac{1}{\sigma}\left(c-\frac{\eta}{(1-u)^{\mu}}\right)\right)du$$

and

$$B(v)=\int\frac{\psi(v)}{vg(v)}\,dv=\int\frac{1}{v}\left(-(\chi+\alpha)+\frac{\rho}{(1-v)^{\delta}}\right)dv, \tag{3.4}$$

it holds that

$$\lim_{u\to 0^+}A(u)=\lim_{u\to 1^-}A(u)=\lim_{v\to 0^+}B(v)=\lim_{v\to 1^-}B(v)=+\infty\,,$$

as required in [18], too. Hence, System (3.1) admits $\widehat{E}(u,v)=A(u)+B(v)$ as first integral having $\widehat{P}$ as minimum point and, according to [18, Theorem 3.1], its solutions are periodic and describe closed orbits, contained in the unit square, around $\widehat{P}$, that is a global center. In symbols, the orbit equations are then given by $\widehat{E}(u,v)=\ell$ for some $\ell\geq\widehat{\ell}_0$, where $\widehat{\ell}_0=\widehat{E}(\widehat{P})$. Although an exhaustive analysis of the period of the orbits of System (3.1) seems not to be easy to perform as discussed in [18] due to the presence of singularities in the model at $u=v=1$, Madotto et al. prove useful results about the period of small and large orbits for System (3.3). Namely, on the one hand, they show that the approximation of the period length of small cycles by means of the period of the linearized system is valid near the equilibrium point (cf. Corollary 5.2 in [18]) and, on the other hand, they prove that the period length of large cycles, approaching the boundary of the feasible set, is arbitrarily high, in the case that f and g are for instance $\mathcal{C}^1$ functions on the open interval $(0,1)$, that are continuous in 0, too (cf. Theorem 5.3 in [18]), like it happens in our framework. As previously mentioned, in view of applying to System (3.1), or more precisely to (3.5) below, the method of the LTMs in some concrete scenarios (cf. Example 3.1), firstly we perturb the center position by supposing that σ alternates in a periodic fashion

between two different levels, due to a seasonal effect, so as to obtain two conservative systems, for which we can find two linked together annuli suitably choosing an annulus made of energy level lines for each system. Then, we will numerically check that the periods of the orbits coinciding with the inner and the outer boundaries of the considered linked annuli do not coincide. Actually, all the numerical simulations that we performed suggest the increasing monotonicity of the period of the orbits for System (3.1) with respect to the energy level, in analogy with the classical results in [34, 38] for the original formulation of the Goodwin model, and in agreement with the numerical simulations reported in [18], even if, to the best of our knowledge, a rigorous proof of the period monotonicity for System (3.1) is not available in the literature. In fact, using a different, more abstract notation, such system has essentially been proposed in [18, Subsection 5.3] to illustrate the difficulties which arise when trying to prove that the period map connected with the general framework analyzed in that paper, described by (3.3), is increasing. The detailed numerical investigations performed in [18] suggest that the desired result holds true for the setting we deal with, even if the period map has a different behavior in the four regions, called quadrants in [18], in which the feasible set $(0,1)^2$ is split by the horizontal and vertical lines passing through the center $\widehat{P}$. In more detail, Figures 3–7 in [18, Subsection 5.3] show that the period is very long and increasing with the energy level in the third quadrant, where both u and v assume low values, while it is decreasing in the first quadrant, and it is not monotone in the second and fourth quadrants.

Let us assume that the capital-output ratio alternates in a T-periodic fashion between the same two positive values considered in Section 2, i.e., $\sigma^{(I)} > \sigma^{(II)}$, for the time intervals $t \in [0, T^{(I)})$ and $t \in [T^{(I)}, T^{(I)} + T^{(II)})$, respectively,[8] with $T = T^{(I)} + T^{(II)}$, where $\sigma^{(II)}$ may be seen as a perturbation of $\sigma^{(I)}$. We can then suppose that we are dealing with the following system with periodic

[8]Indeed, the values of $\sigma^{(i)}$ and $T^{(i)}$, for $i \in \{I, II\}$, are determined by the economic features of the capital-output ratio, rather than by the model formulation. Nonetheless, considering different values for $\sigma^{(i)}$ and $T^{(i)}$ with respect to Section 2 would not affect the way in which the LTMs can be applied and the conclusions that it allows to draw, as long as $0 < \sigma^{(II)} < \sigma^{(I)}$ and $T^{(I)}$, $T^{(II)}$ are large enough.

coefficients

$$\begin{cases} u' = u\left(-(\chi(t)+\alpha(t)) + \frac{\rho(t)}{(1-v)^{\delta(t)}}\right) \\ v' = v\left(-(\alpha(t)+\beta(t)) + \frac{1}{\sigma(t)}\left(c(t) - \frac{\eta(t)}{(1-u)^{\mu(t)}}\right)\right) \end{cases} \tag{3.5}$$

in which $\kappa(t)$ coincides with κ, for $\kappa \in \{\alpha, \beta, \chi, c, \delta, \eta, \mu, \rho\}$, $\sigma(t)$ is as in (2.5), assuming to have extended it to the whole real line by T-periodicity, and

$$0 < \sigma^{(II)} < \sigma^{(I)} < \frac{c-\eta}{\alpha+\beta}, \quad \rho < \chi + \alpha, \quad \delta \geq 1, \quad \mu \geq 1 \tag{3.6}$$

as a consequence of (3.2).
Calling (Mi), where M stands for "Modified (version of the Goodwin model)", the system that we obtain when the capital-output ratio takes value $\sigma^{(i)}$, for $i \in \{I, II\}$, it is conservative, with the center coinciding with

$$\widehat{P}^{(i)} = \left(1 - \left(\frac{\eta}{c - \sigma^{(i)}(\alpha+\beta)}\right)^{\frac{1}{\mu}}, 1 - \left(\frac{\rho}{\chi+\alpha}\right)^{\frac{1}{\delta}}\right). \tag{3.7}$$

Similar to what happened in Section 2, passing from $\widehat{P}^{(I)}$ to $\widehat{P}^{(II)}$ the abscissa of the center raises, while its ordinate does not change. The orbits of Systems (MI) and (MII) are closed, surrounding the corresponding center, and a straightforward analysis of the phase portrait shows that they are run clockwise (cf. Figure 2 (A)). Setting $A^{(i)}(u) = \int \frac{1}{u}\left((\alpha+\beta) - \frac{1}{\sigma^{(i)}}\left(c - \frac{\eta}{(1-u)^{\mu}}\right)\right) du$, for $i \in \{I, II\}$, and recalling the definition of $B(v)$ in (3.4), the orbits of Systems (MI) and (MII) have respectively equation $\widehat{E}^{(I)}(u,v) = A^{(I)}(u) + B(v) = \ell$ for some $\ell \geq \widehat{\ell}_0^{(I)} = \widehat{E}^{(I)}(\widehat{P}^{(I)})$ and $\widehat{E}^{(II)}(u,v) = A^{(II)}(u) + B(v) = h$ for some $h \geq \widehat{h}_0^{(II)} = \widehat{E}^{(II)}(\widehat{P}^{(II)})$. The sets $\widehat{\Gamma}^{(I)}(\ell)$ and $\widehat{\Gamma}^{(II)}(h)$ can then be defined like in Section 2 for $\ell > \widehat{\ell}_0^{(I)}$ and $h > \widehat{h}_0^{(II)}$, just replacing $E^{(i)}$ with $\widehat{E}^{(i)}$ for $i \in \{I, II\}$, and they are still simple closed curves surrounding $\widehat{P}^{(I)}$ and $\widehat{P}^{(II)}$, respectively. We can proceed analogously to Section 2 in defining the annuli $\widehat{\mathcal{C}}^{(I)}(\ell_1, \ell_2)$ around $\widehat{P}^{(I)}$, with $\widehat{\ell}_0^{(I)} < \ell_1 < \ell_2$, for System (MI) and $\widehat{\mathcal{C}}^{(II)}(h_1, h_2)$ around $\widehat{P}^{(II)}$, with $\widehat{h}_0^{(II)} < h_1 < h_2$, for System (MII), too. Notice however that, differently from Section 2, we do not need to consider energy levels close to $\widehat{\ell}_0^{(I)}$ and $\widehat{h}_0^{(II)}$ to have annuli for Systems (MI) and (MII) contained in $(0,1)^2$, thanks to the above recalled results obtained in

[18] (cf. in particular Theorem 3.1 therein). Due to the similar effect produced by a variation in σ on the center position for Systems (2.1) and (3.1), the definition of linked together annuli in the new context is analogous to that introduced in Definition 2.1 as well, being based on the same ordering relation $\lhd$, this time on the straight line $\widehat{r}$ joining $\widehat{P}^{(I)}$ and $\widehat{P}^{(II)}$, which has equation $v = 1 - \left(\frac{\rho}{\chi+\alpha}\right)^{\frac{1}{\delta}}$. See Figure 2 (B) for a graphical illustration of two linked annuli $\widehat{\mathcal{C}}^{(I)}(\ell_1, \ell_2)$ and $\widehat{\mathcal{C}}^{(II)}(h_1, h_2)$ for System (3.5). We stress that also in the present framework their boundary sets $\widehat{\Gamma}^{(I)}(\ell_j)$ and $\widehat{\Gamma}^{(II)}(h_j)$, with $j \in \{1, 2\}$, intersect the straight line $\widehat{r}$ in exactly two points because the functions $\widehat{E}^{(I)}$ and $\widehat{E}^{(II)}$ are convex. Namely, their second derivative is non-negative under (3.6) because $(1-z)^\nu > (1 - z(\nu+1))$, $\forall z \in [0,1]$, $\forall \nu > 0$, where in our case $z \in \{u, v\}$ and $\nu \in \{\mu + 1, \delta + 1\}$, respectively. In view

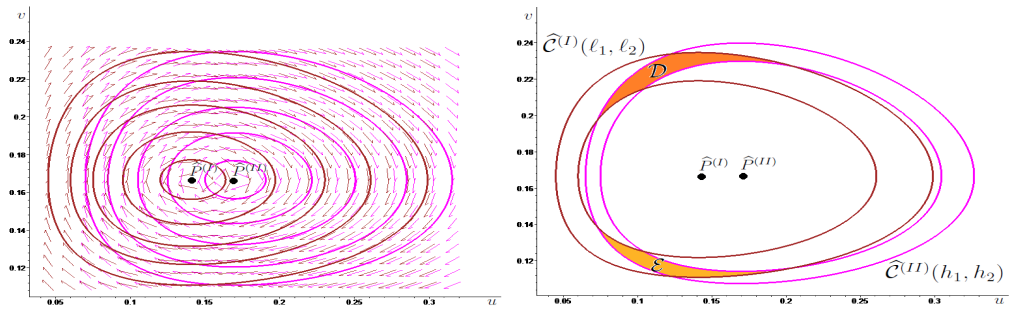

(A) (B)

Figure 2: In (A) we draw in brown some energy level lines associated with System (MI), around $\widehat{P}^{(I)}$, and in magenta some energy level lines associated with System (MII), around $\widehat{P}^{(II)}$, showing also the corresponding phase portrait. In (B), we illustrate two linked together annuli, that we call $\widehat{\mathcal{C}}^{(I)}(\ell_1, \ell_2)$ and $\widehat{\mathcal{C}}^{(II)}(h_1, h_2)$, obtained by suitably choosing two level lines for each system, as well as the two disjoint generalized rectangles $\mathcal{D}$ (colored in dark orange) and $\mathcal{E}$ (colored in light orange) where the annuli meet.

of stating our result about System (3.5) (cf. Proposition 3.1 below), for which we will not provide a proof due to its similarity with the verification of Proposition 2.1, we introduce the Poincaré map $\widehat{\Psi}$ associated with System (3.5), that can be decomposed as $\widehat{\Psi} = \widehat{\Psi}^{(II)} \circ \widehat{\Psi}^{(I)}$, where $\widehat{\Psi}^{(I)}$ is the Poincaré map associated with System (MI) for $t \in [0, T^{(I)}]$ and $\widehat{\Psi}^{(II)}$ is the Poincaré

map associated with System (MII) for $t \in [0, T^{(II)}]$. Notice that every pair of linked together annuli for System (3.5), being made of energy level lines of Systems (Mi), $i \in \{I, II\}$, are invariant under the action of $\widehat{\Psi}$. We denote by $\widehat{\tau}^{(I)}(\ell)$, for all $\ell > \widehat{\ell}_0^{(I)}$, the period of $\widehat{\Gamma}^{(I)}(\ell)$, and by $\widehat{\tau}^{(II)}(h)$, for all $h > \widehat{h}_0^{(II)}$, the period of $\widehat{\Gamma}^{(II)}(h)$, recalling that the period of an orbit is the time needed by the solution to the considered system, starting from a certain point of the orbit, to complete one turn around the corresponding center, moving around the orbit itself. As discussed above, the increasing monotonicity of $\widehat{\tau}^{(I)}(\,\cdot\,)$ and $\widehat{\tau}^{(II)}(\,\cdot\,)$ with the energy levels is suggested by the many simulative experiments that we performed and by the accurate numerical analysis in [18, Subsection 5.3], but, to the best of our knowledge, a rigorous proof is not available in the literature. In the absence of a result showing that the period of orbits of Systems (MI) and (MII) always increases with energy levels, in Proposition 3.1 we assume that, given two linked together annuli for System (3.5), the period of the orbits composing their inner boundary is smaller than the period of the orbits composing their outer boundary. The main difference between Propositions 2.1 and 3.1 lies indeed in the necessity to exclude in the latter that the period remains unchanged between the inner and outer boundaries of the linked annuli, since a variation in the periods is required for the Poincaré map to produce a twist effect on the annuli, which in turn allows to apply the LTMs method. We recall that for System (2.4) such a variation was granted by the results in [34, 38] on the monotonicity of the period of orbits for the Lotka-Volterra predator-prey model.

Proposition 3.1 *For any choice of the positive parameters $\alpha, \beta, \chi, c, \delta, \eta, \mu, \rho$, $\widehat{\sigma}^{(I)}, \widehat{\sigma}^{(II)}$ satisfying* (3.6)*, given the annulus $\widehat{\mathcal{C}}^{(I)}(\ell_1, \ell_2)$ around $\widehat{P}^{(I)}$, for some $\widehat{\ell}_0^{(I)} < \ell_1 < \ell_2$, and the annulus $\widehat{\mathcal{C}}^{(II)}(h_1, h_2)$ around $\widehat{P}^{(II)}$, for some $\widehat{h}_0^{(II)} < h_1 < h_2$, assume that they are linked together, calling $\mathcal{D}$ and $\mathcal{E}$ the connected components of $\widehat{\mathcal{C}}^{(I)}(\ell_1, \ell_2) \cap \widehat{\mathcal{C}}^{(II)}(h_1, h_2)$. Then, if $\widehat{\tau}^{(I)}(\ell_1) < \widehat{\tau}^{(I)}(\ell_2)$, $\widehat{\tau}^{(II)}(h_1) < \widehat{\tau}^{(II)}(h_2)$, it holds that for every $\widehat{m}^{(I)} \geq 1$ and $\widehat{m}^{(II)} \geq 1$ with $\widehat{m} = \widehat{m}^{(I)}\widehat{m}^{(II)} \geq 2$ there exist two positive constants $\widehat{t}^{(I)} = \widehat{t}^{(I)}(\widehat{m}^{(I)}, \widehat{\tau}^{(I)}(\ell_1), \widehat{\tau}^{(I)}(\ell_2))$ and $\widehat{t}^{(II)} = \widehat{t}^{(II)}(\widehat{m}^{(II)}, \widehat{\tau}^{(II)}(h_1), \widehat{\tau}^{(II)}(h_2))$ such that if $T^{(i)} > \widehat{t}^{(i)}$, for $i \in \{I, II\}$, the Poincaré map $\widehat{\Psi} = \widehat{\Psi}^{(II)} \circ \widehat{\Psi}^{(I)}$ of System* (3.5) *induces chaotic dynamics on $\widehat{m}$ symbols in $\mathcal{D}$ and in $\mathcal{E}$, and all the properties listed in Theorem 4.1 are fulfilled for $\widehat{\Psi}$.*

We remark that the same conclusions in Proposition 3.1 would hold true also if the period of the inner boundary were larger (rather than smaller) with

respect to the period of the outer boundary for at least one of the linked together annuli.[9] In Proposition 3.1 we chose to focus on the framework in which the period of the inner boundary is smaller than the period of the outer boundary for both the linked together annuli because this is the scenario observed in the numerical experiments in [18, Subsection 5.3], as well as in all the simulations that we performed. We find that same framework in Example 3.1, too, that concludes the present investigation of the modified version of the Goodwin model by illustrating a numerical context, in which Proposition 3.1 can be applied to show the existence of chaotic dynamics.
Notice that the parameter configuration considered in Example 3.1 and in its illustration in Figure 2 coincides with that used to draw Figure 1 in Section 2, as well as Figures 3 and 4 in the Appendix, except for the parameters c, δ, η and μ, which were not present in the model original formulation in (2.1), and for the parameters χ and ρ, whose values have now been interchanged, in order to satisfy the second condition in (3.6), i.e., $\rho < \alpha + \chi$, guaranteeing that the ordinate of the centers for System (3.5) lies in the interval $(0, 1)$. Namely, such hypothesis is incompatible with the last condition in (2.6), which played the same role in regard to the ordinate of the centers for System (2.4). Hence, some differences in the parameter values for the original and the modified versions of the Goodwin model need to be introduced, but we will avoid adding unnecessary ones. In regard to the new parameters δ and μ, we will deal with the same values, i.e. $\delta = 1$ and $\mu = 1.2$, used in the numerical simulations performed in [18, Subsection 5.3] where, as already recalled, the authors illustrate the issues which arise when trying to prove that the period map connected with System (3.1) is increasing, even if they find numerical evidence of such conjecture for the above values of δ and μ. We stress that the case $\delta = 1$ was also considered in [8] (cf. page 2668 therein), although in that framework the parameter μ was not present.

Example 3.1 *Taking* $\alpha = 0.02$, $\beta = 0.01$, $\chi = 0.7$, $\rho = 0.6$, $\sigma^{(I)} = 3$, $\sigma^{(II)} = 2.5$, $c = 0.45$, $\eta = 0.3$, $\delta = 1$, $\mu = 1.2$ *and recalling* (3.7)*, System* (MI) *has a center in* $\widehat{P}^{(I)} = (0.141, 0.167)$ *while System* (MII) *has a center in* $\widehat{P}^{(II)} = (0.170, 0.167)$.
As shown in Figure 2 (B), two linked together annuli $\widehat{\mathcal{C}}^{(I)}(e_1, e_2)$ *and* $\widehat{\mathcal{C}}^{(II)}(h_1,$

[9]Notice that in those cases the position of the boundary periods should be exchanged on the denominator of the fractions defining $\widehat{t}^{(I)}$ and/or $\widehat{t}^{(II)}$, which respectively coincide with those for $t^{(I)}$ and $t^{(II)}$ in the proof of Proposition 2.1 (see the Appendix), when replacing $\tau^{(i)}$ with $\widehat{\tau}^{(i)}$, for $i \in \{I, II\}$.

h_2) *can be obtained for* $e_1 = 0.8657$, $e_2 = 0.8696$, $h_1 = 0.9865$, $h_2 = 0.9892$, *intersecting in the two disjoint generalized rectangles denoted by* $\mathcal{D}$ *and* $\mathcal{E}$. *Software-assisted computations show that* $\widehat{\tau}^{(I)}(e_1) \approx 111 < \widehat{\tau}^{(I)}(e_2) \approx 114$ *and* $\widehat{\tau}^{(II)}(h_1) \approx 89 < \widehat{\tau}^{(II)}(h_2) \approx 90$. *Hence, Proposition 3.1 guarantees the existence of chaotic dynamics for the Poincaré map* $\widehat{\Psi} = \widehat{\Psi}^{(II)} \circ \widehat{\Psi}^{(I)}$ *associated with System* (3.5) *provided that the switching times* $\widehat{T}^{(I)}$ *and* $\widehat{T}^{(II)}$ *are large enough.*

4 Recalling the Linked Twist Maps method

In the present section we briefly recall the planar results about the Linked Twist Maps (LTMs) method that we have used in Sections 2 and 3, referring the interested reader to [24, 30] for further details and to [35] for a three-dimensional version of it.

Although in the literature different assumptions, connected e.g. with measure theory and differential calculus, have been made on linked twist maps (see e.g. [5, 31, 32]), we just rely on topological hypotheses. Indeed, given two annuli crossing along two (or more) planar sets homeomorphic to the unit square, by a linked twist map we mean the composition of two twist maps, each acting on one of the two annuli, which are homeomorphisms and that, similar to what required in the Poincaré-Birkhoff fixed point theorem, produce a twist effect on the boundary sets of the two annuli, leaving them invariant. In the applications of LTMs illustrated in the present paper, we have analyzed Hamiltonian systems with a nonisochronous center, whose position varies when modifying a parameter for which it is sensible to assume, due to a seasonal effect, a periodic alternation between two different values, one of which may be seen as a perturbation of the other. Thanks to this alternation, we obtain two conservative systems with a nonisochronous center and for each of them we can consider an annulus composed of energy level lines. Under certain conditions on the orbits, the two annuli cross in two generalized rectangles. The LTMs method consists in proving the presence of chaotic dynamics for the Poincaré map obtained as composition of the Poincaré maps associated with the unperturbed system and with the perturbed one, which are homeomorphisms, by checking that they satisfy suitable stretching relations (cf. conditions (C_F) and (C_G) in Theorem 4.1, as well as (4.1)). We stress that the nonisochronicity of the centers is crucial in the above described procedure, because it implies that the orbits composing the linked annuli are

run with a different speed, so that the Poincaré maps produce a twist effect on the linked annuli, despite the invariance of closed orbits under the action of the Poincaré maps.
The stretching relation in (4.1) is the kernel of the Stretching Along the Paths (henceforth, SAP) method, i.e. the topological technique, developed in the planar case in [21, 22] and extended to the N-dimensional framework in [29], that allows to show the existence of fixed points, periodic points and chaotic dynamics for continuous maps that expand the arcs along one direction and that are defined on sets homeomorphic to the unit square. We start by introducing its main aspects, in order to be able to state Theorem 4.1, so that we can then more precisely describe what we mean by chaos.
We call *path* in $\mathbb{R}^2$ any continuous function $\gamma : [0,1] \to \mathbb{R}^2$ and we set $\overline{\gamma} := \gamma([0,1])$. By a *generalized rectangle* we mean a subset $\mathcal{R}$ of $\mathbb{R}^2$ homeomorphic to the unit square $[0,1]^2$, through a homeomorphism $H : \mathbb{R}^2 \supseteq [0,1]^2 \to \mathcal{R} \subseteq \mathbb{R}^2$. We also introduce the *left* and the *right sides* of $\mathcal{R}$, defined respectively as $\mathcal{R}_l^- := H(\{0\} \times [0,1])$ and $\mathcal{R}_r^- := H(\{1\} \times [0,1])$. We call the pair

$$\widetilde{\mathcal{R}} := (\mathcal{R}, \mathcal{R}^-)$$

an *oriented rectangle of* $\mathbb{R}^2$, where $\mathcal{R}^- := \mathcal{R}_l^- \cup \mathcal{R}_r^-$.
The *stretching along the paths* relation for maps between oriented rectangles can then be defined as follows:

Definition 4.1 *Given* $\widetilde{\mathcal{N}} := (\mathcal{N}, \mathcal{N}^-)$ *and* $\widetilde{\mathcal{O}} := (\mathcal{O}, \mathcal{O}^-)$ *oriented rectangles of* $\mathbb{R}^2$, *let* $F : \mathcal{N} \to \mathbb{R}^2$ *be a function and* $\mathcal{H} \subseteq \mathcal{N}$ *be a compact set. We say that* $(\mathcal{H}, F)$ *stretches* $\widetilde{\mathcal{N}}$ *to* $\widetilde{\mathcal{O}}$ *along the paths, and write*

$$(\mathcal{H}, F) : \widetilde{\mathcal{N}} \twoheadrightarrow \widetilde{\mathcal{O}}, \tag{4.1}$$

if

- F *is continuous on* $\mathcal{H}$;
- *for every path* $\gamma : [0,1] \to \mathcal{N}$ *with* $\gamma(0) \in \mathcal{N}_l^-$ *and* $\gamma(1) \in \mathcal{N}_r^-$ *or with* $\gamma(0) \in \mathcal{N}_r^-$ *and* $\gamma(1) \in \mathcal{N}_l^-$ *there exists* $[t', t''] \subseteq [0,1]$ *such that* $\gamma([t', t'']) \subseteq \mathcal{H}$, $F \circ \gamma([t', t'']) \subseteq \mathcal{O}$, *with* $F(\gamma(t')) \in \mathcal{O}_l^-$ *and* $F(\gamma(t'')) \in \mathcal{O}_r^-$ *or with* $F(\gamma(t')) \in \mathcal{O}_r^-$ *and* $F(\gamma(t'')) \in \mathcal{O}_l^-$.

We stress that to check the stretching relation in (4.1) we may need to consider paths $\gamma : [0,1] \to \mathcal{N}$ with $\gamma(0) \in \mathcal{N}_r^-$ and $\gamma(1) \in \mathcal{N}_l^-$ e.g. when dealing

with the composition of two functions (like in (4.2) where $\Phi := G \circ F$), since it can happen that the image through the first map of paths joining the opposite sides of a certain oriented rectangle $\widetilde{\mathcal{M}}$ from left to right connects the sides of $\mathcal{N}^-$ from right to left through a path that is the starting point of the second function. Nonetheless in the proof of Proposition 2.1, contained in the Appendix, it will suffice for us to focus on paths joining the left and the right sides of the generalized rectangles where the functions start from, since we will not directly deal with composite mappings. Namely, thanks to Theorem 4.1 (cf. in particular (C_F) and (C_G) therein), in order to check the existence of chaotic dynamics for the Poincaré map obtained as composition of the Poincaré maps associated with the unperturbed Hamiltonian system and with the perturbed one, we can deal with those two Poincaré maps separately.

Theorem 4.1 *Let $F : \mathbb{R}^2 \supseteq D_F \to \mathbb{R}^2$ and $G : \mathbb{R}^2 \supseteq D_G \to \mathbb{R}^2$ be continuous maps defined on the sets D_F and D_G, respectively. Let also $\widetilde{\mathcal{N}} := (\mathcal{N}, \mathcal{N}^-)$ and $\widetilde{\mathcal{O}} := (\mathcal{O}, \mathcal{O}^-)$ be oriented rectangles of $\mathbb{R}^2$. Suppose that the following conditions are satisfied:*

(C_F) *there are $\widehat{m} \geq 1$ pairwise disjoint compact sets $\mathcal{H}_0, \dots, \mathcal{H}_{\widehat{m}-1} \subseteq \mathcal{N} \cap D_F$ such that $(\mathcal{H}_i, F) : \widetilde{\mathcal{N}} \twoheadrightarrow \widetilde{\mathcal{O}}$, for $i = 0, \dots, \widehat{m} - 1$;*

(C_G) *there are $\breve{m} \geq 1$ pairwise disjoint compact sets $\mathcal{K}_0, \dots, \mathcal{K}_{\breve{m}-1} \subseteq \mathcal{O} \cap D_G$ such that $(\mathcal{K}_j, G) : \widetilde{\mathcal{O}} \twoheadrightarrow \widetilde{\mathcal{N}}$, for $j = 0, \dots, \breve{m} - 1$;*

(C_m) *$m := \widehat{m} \cdot \breve{m} \geq 2$;*

(C_Φ) *the composite map $\Phi := G \circ F$ is injective on*

$$\mathcal{H}^* := \bigcup_{\substack{i = 0, \dots, \widehat{m} - 1 \\ j = 0, \dots, \breve{m} - 1}} \mathcal{H}'_{i,j}\,, \quad \text{with } \mathcal{H}'_{i,j} := \mathcal{H}_i \cap F^{-1}(\mathcal{K}_j)\,.$$

Then, setting

$$X_\infty := \bigcap_{n=-\infty}^{\infty} \Phi^{-n}(\mathcal{H}^*),$$

there exists a nonempty compact set

$$X \subseteq X_\infty \subseteq \mathcal{H}^*$$

on which the following properties are fulfilled:

(*i*) *X is invariant for Φ (that is, $\Phi(X) = X$);*

(*ii*) *$\Phi \restriction_X$ is semi-conjugate to the two-sided Bernoulli shift on m symbols, i.e., there exists a continuous map π from X onto $\Sigma_m := \{0, \dots, m-1\}^{\mathbb{Z}}$, endowed with the distance*

$$d(\boldsymbol{s}', \boldsymbol{s}'') := \sum_{i \in \mathbb{Z}} \frac{|s'_i - s''_i|}{m^{|i|+1}},$$

for $\boldsymbol{s}' = (s'_i)_{i\in\mathbb{Z}}$ and $\boldsymbol{s}'' = (s''_i)_{i\in\mathbb{Z}} \in \Sigma_m$, such that the diagram

$$\begin{array}{ccc} X & \xrightarrow{\Phi} & X \\ {\scriptstyle\pi}\downarrow & & \downarrow{\scriptstyle\pi} \\ \Sigma_m & \xrightarrow[\sigma]{} & \Sigma_m \end{array}$$

commutes, i.e. $\pi \circ \Phi = \sigma \circ \pi$, where $\sigma : \Sigma_m \to \Sigma_m$ is the Bernoulli shift defined by $\sigma((s_i)_i) := (s_{i+1})_i$, $\forall i \in \mathbb{Z}$;

(*iii*) *the set $\mathcal{P}$ of the periodic points of $\Phi \restriction_{X_\infty}$ is dense in X and the preimage $\pi^{-1}(\boldsymbol{s}) \subseteq X$ of every k-periodic sequence $\boldsymbol{s} = (s_i)_{i\in\mathbb{Z}} \in \Sigma_m$ contains at least one k-periodic point.*

Furthermore, from conclusion (ii) it follows that:

(*iv*)
$$h_{\text{top}}(\Phi) \geq h_{\text{top}}(\Phi \restriction_X) \geq h_{\text{top}}(\sigma) = \log(m),$$
where h_{top} is the topological entropy;

(*v*) *there exists a compact invariant set $\Lambda \subseteq X$ such that $\Phi|_\Lambda$ is semi-conjugate to the two-sided Bernoulli shift on m symbols, topologically transitive and displays sensitive dependence on initial conditions.*

Proof. The crucial step consists in showing that

$$(\mathcal{H}'_{i,j}, \Phi) : \widetilde{\mathcal{N}} \twoheadrightarrow \widetilde{\mathcal{N}}\,,\ i = 0, \dots, \widehat{m} - 1,\ j = 0, \dots, \breve{m} - 1. \tag{4.2}$$

See Theorem 3.1 in [23] for a verification of this property in more general spaces for the case $\widehat{m} = m \geq 2$, $\breve{m} = 1$. The condition in (4.2) is then easy to

check (cf. Theorem 3.2 in [23] for a result analogous to ours, which follows as a corollary from Theorem 3.1 therein).
Recalling Definition 2.3 in [23], as a consequence of (4.2) it holds that Φ *induces chaotic dynamics on* m *symbols* in the set $\mathcal{N}$. Conclusions (i)–(v) follow then by Theorem 2.2 and by Footnote 4 in [20], where however the case $m = 2$ is considered.

In the proof of Theorem 4.1, we mentioned the concept of a map inducing chaotic dynamics on $m \geq 2$ symbols on a set according to Definition 2.3 in [23]. Even if for brevity's sake we will not go into detail, we just stress that such notion of chaos for the case $m = 2$ bears a deep resemblance to the concept of chaos in the coin-tossing sense discussed in [15], being however stronger than it. Namely, in addition to the requirement in [15] that every two-sided sequence of two symbols is realized through the iterates of the map, jumping between two disjoint compact subsets, Definition 2.3 in [23] also requires periodic sequences of symbols to be reproduced by periodic orbits of the map. We refer the interested reader to [20] for a comparison with other notions of chaos widely considered in the literature.
Notice that, in the light of [23, Definition 2.3], we can rephrase the statement of Theorem 4.1 above by saying that, when conditions (C_F), (C_G), (C_m) and (C_Φ) therein are satisfied, the composite map $\Phi = G \circ F$ induces chaotic dynamics on $m \geq 2$ symbols in $\mathcal{N}$, knowing that from this fact all the properties listed in Theorem 4.1 hold true for $G \circ F$, in regard to the existence of periodic points, too. We indeed used such reformulation of Theorem 4.1 in Sections 2 and 3 (see for instance the statement of Propositions 2.1 and 3.1) when dealing with the composition of the Poincaré maps associated with the unperturbed and with the perturbed Hamiltonian systems.

5 Concluding remarks

In the present work, following the seminal idea by Goodwin in [13] of studying forced models in economics, obtained superimposing exogenous cycles to cycles endogenously generated by a model, we showed the existence of complex dynamics in both the original version of his celebrated growth cycle model (see [11, 12]), and for a modified formulation of it, encompassing nonlinear expressions of the real wage bargaining function and of the investment function, already considered in the literature. In particular, in regard to the real wage bargaining function we dealt with the formulation proposed by Phillips

in [27], while for the investment function we used an expression employed in [18]. The need to consider a modified formulation of the Goodwin model was motivated by the observation that its original version does not guarantee that orbits lie in the unit square, as they should, since the state variables are wage share in national income and proportion of labor force employed, which can neither be negative, nor exceed unity. We however underline that a nonlinear investment function is grounded also from an economic viewpoint since it encompasses a description of a more flexible savings behavior (cf. [9, 39]) and that Goodwin initially considered the nonlinear version of the Phillips curve in [27], then linearizing it so as to obtain an approximation "*in the interest of lucidity and ease of analysis*" [11, page 55].

Exploiting in both the original and the modified settings the periodic dependence on time of one of the model parameters and the Hamiltonian structure, characterized by the presence of a global nonisochronous center, we proved the presence of chaos for the Poincaré map associated with the considered systems by means of the Linked Twist Maps (LTMs) method, used e.g. in [24, 30]. This led us to work with discrete-time dynamical systems. We stress that the obtained results, in their general conclusions, do not depend on the particular expression of the equations involved, as long as we enter e.g. the class of Hamiltonian systems considered in [18], for which it is therein proven that the center is nonisochronous and that orbits lie in the unit square. Concerning the needed economic assumptions, we recall that the real wage bargaining function has to be increasing in the proportion of labor force employed, while the investment function has to be decreasing in wage share in national income.

Despite the issue with the orbit position in the original Goodwin model, even for that formulation we have been able to prove the existence of chaotic sets lying in the unit square thanks to the features of the LTMs method. Namely, the chaotic sets are located inside the generalized rectangular regions obtained as intersection of the detected pair of linked annuli, that jointly constitute an invariant set under the action of the composite Poincaré map. Indeed each annulus, being made of periodic orbits, is invariant under the action of the Poincaré map describing the corresponding regime. Choosing then linked together annuli contained in the unit square solves the problem. As our illustrative examples showed, this can be done even when dealing with parameter configurations analogous to those considered in [8, 14].

The seminal idea by Goodwin in [13] of studying forced models in economics has been recently applied to a three-dimensional setting in [7], where the au-

thors investigate the implications of describing exports as a function of the capital stock in the framework introduced in [6], which extends the original Goodwin model in [11] to an open economy setting that includes the balance-of-payments constraint (BoPC) on growth. In more detail, in agreement with Goodwin's insight in [10] that Schumpeterian innovations requiring investment occur periodically, the authors in [7] add a nonlinear forcing term in the capital accumulation function and, referring to their Fig. 5 on page 266, say that "*In this way, we obtain a scenario in which a non-linear system with a "natural" oscillation frequency interacts with an external "force" resulting in a chaotic attractor as shown in Fig. 5. The interplay between two or more independent frequencies characterising the dynamics of the system is a well-known route to more complex behaviour*". It would then be interesting to check whether the LTMs method, or more generally the SAP (Stretching Along the Paths) technique, on which the LTMs method is based, could be employed in that setting, too, in order to rigorously prove the existence of complex dynamics.

In regard to three-dimensional applications of the LTMs technique, we recall [35] where, dealing with linked together cylindrical sets, the focus is on a 3D non-Hamiltonian system describing a predator-prey model with a Beddington-DeAngelis functional response in a periodically varying environment. Related to this, we also mention the 3D continuous-time non-Hamiltonian framework representing the Lotka-Volterra model with two predators and one prey in a periodic environment considered in [36], for which the presence of chaos has been shown by means of the SAP technique, without relying on the LTMs geometry. Despite such dissimilarity in the employed method, the common starting point in the proofs of chaos for the frameworks analyzed in [35, 36] is given by a study of the properties of the classical planar Lotka-Volterra system. Since, as we have seen, Goodwin growth cycle model in [11, 12] is a special case of the predator-prey setting, in view of proving the existence of chaotic phenomena for its 3D extension proposed in [7], we could try to apply similar arguments to those used in [35, 36]. We will investigate this possibility in a future work.

Funding: This research received no external funding.

Acknowledgments: Many thanks to Professor Ahmad Naimzada for helpful conversations about the Goodwin model and to Professor Fabio Zanolin for interesting discussions about the state of the art in applications of the Linked Twist Maps method.

Conflicts of Interest: The author declares no conflict of interest.

References

[1] J. Alvarez-Ramirez, R. Escarela-Perez, G. Espinosa-Perez and R. Urrea, Dynamics of electricity market correlations, Physica A 388 (2009), 2173–2188.

[2] S. Arango and E. Larsen, Cycles in deregulated electricity markets: Empirical evidence from two decades, Energy Policy 39 (2011), 2457–2466.

[3] M. Braun, "Differential Equations and Their Applications. An introduction to Applied Mathematics," 4th ed., Texts in Applied Mathematics, 11. Springer-Verlag, New York, 1993.

[4] L. Burra and F.Zanolin, Chaotic dynamics in a vertically driven planar pendulum, Nonlinear Anal. 72 (2010), 1462–1476.

[5] R. Burton and R. W. Easton, Ergodicity of linked twist maps, in "Global Theory of Dynamical Systems," Proc. Int. Conf., Northwestern Univ., Evanston, Ill., 1979, Lecture Notes in Math., 819. Springer, Berlin, (1980), 35–49.

[6] M. J. Dávila-Fernández and S. Sordi, Distributive cycles and endogenous technical change in a BoPC growth model, Econ. Model. 77 (2019), 216–233.

[7] M. J. Dávila-Fernández and S. Sordi, Path dependence, distributive cycles and export capacity in a BoPC growth model, Struct. Change Econ. Dyn. 50 (2019), 258–272.

[8] M. Desai, B. Henry, A. Mosley and M. Pemberton, A clarification of the Goodwin model of the growth cycle, J. Econ. Dyn. Control 30 (2006), 2661–2670.

[9] P. Flaschel, Some stability properties of Goodwin's growth cycle. A critical elaboration, Z. Nationalökon. 44 (1984), 63–69.

[10] R. Goodwin, The nonlinear accelerator and the persistence of business cycles, Econometrica 19 (1951), 1–17.

[11] R. M. Goodwin, A growth cycle, in "Socialism, Capitalism and Economic Growth" (ed. C. H. Feinstein), Cambridge University Press, Cambridge, (1967), 54–58.

[12] R. M. Goodwin, A growth cycle, in "A Critique of Economic Theory" (eds. E. K. Hunt and J. G. Schwartz), Penguin, Harmondsworth, (1972), 442–449.

[13] R. M. Goodwin, "Chaotic Economic Dynamics," Oxford University Press, Oxford, 1990.

[14] D. Harvie, M. A. Kelmanson and D. G. Knapp, A dynamical model of business-cycle asymmetries: Extending Goodwin, Econ. Issues 12 (2007), 53–92.

[15] U. Kirchgraber and D. Stoffer, On the definition of chaos, Z. Angew. Math. Mech. 69 (1989), 175–185.

[16] M. A. Krasnosel'skiĭ, "The Operator of Translation Along the Trajectories of Differential Equations," Translations of Mathematical Monographs, 19. American Mathematical Society, Providence, 1968.

[17] L. A. Lillard and J. P. Acton, Seasonal electricity demand and pricing analysis with a variable response model, Bell J. Econ. 12 (1981), 71–92.

[18] M. Madotto, M. Gaudenzi and F. Zanolin, A generalized approach for the modeling of Goodwin-type cycles, Adv. Nonlinear Stud. 16 (2016), 775–793.

[19] A. Margheri, C. Rebelo and F. Zanolin, Chaos in periodically perturbed planar Hamiltonian systems using linked twist maps, J. Differ. Equ. 249 (2010), 3233–3257.

[20] A. Medio, M. Pireddu and F. Zanolin, Chaotic dynamics for maps in one and two dimensions: a geometrical method and applications to economics, Int. J. Bifurc. Chaos Appl. Sci. Eng. 19 (2009), 3283–3309.

[21] D. Papini and F. Zanolin, On the periodic boundary value problem and chaotic-like dynamics for nonlinear Hill's equations, Adv. Nonlinear Stud. 4 (2004), 71–91.

[22] D. Papini and F. Zanolin, Fixed points, periodic points, and coin-tossing sequences for mappings defined on two-dimensional cells, Fixed Point Theory Appl. 2004 (2004), 113–134.

[23] A. Pascoletti, M. Pireddu and F. Zanolin, Multiple periodic solutions and complex dynamics for second order ODEs via linked twist maps, Electron. J. Qual. Theory Differ. Equ., Proc. 8th Colloq. Qual. Theory Differ. Equ. 14 (2008), 1–32.

[24] A. Pascoletti and F. Zanolin, Example of a suspension bridge ODE model exhibiting chaotic dynamics: A topological approach, J. Math. Anal. Appl. 339 (2008), 1179–1198.

[25] A. Pascoletti and F. Zanolin, Chaotic dynamics in periodically forced asymmetric ordinary differential equations, J. Math. Anal. Appl. 352 (2009), 890–906.

[26] A. Pascoletti and F. Zanolin, From the Poincaré-Birkhoff fixed point theorem to linked twist maps: Some applications to planar Hamiltonian systems, in "Differential and Difference Equations with Applications" (eds. S. Pinelas, M. Chipot and Z. Dosla), Springer Proceedings in Mathematics & Statistics, 47. Springer, New York, (2013), 197–213.

[27] A. W. H. Phillips, The relationship between unemployment and the rate of change of money wage rates in the United Kingdom, 1861–1957, Economica 25(NS) (1958), 283–299.

[28] M. Pireddu, Chaotic dynamics in the presence of medical malpractice litigation: A topological proof via linked twist maps for two evolutionary game theoretic contexts, J. Math. Anal. Appl. 501 (2021), 125224.

[29] M. Pireddu and F. Zanolin, Cutting surfaces and applications to periodic points and chaotic-like dynamics, Topol. Methods Nonlinear Anal. 30 (2007), 279–319. Topol. Methods Nonlinear Anal. 33 (2009), 395, erratum.

[30] M. Pireddu and F. Zanolin, Chaotic dynamics in the Volterra predator-prey model via linked twist maps, Opuscula Mathematica 28/4 (2008), 567–592.

[31] F. Przytycki, Ergodicity of toral linked twist mappings, Ann. Sci. École Norm. Super. 16 (1983), 345–354.

[32] F. Przytycki, Periodic points of linked twist mappings, Stud. Math. 83 (1986), 1–18.

[33] O. E. Rössler, An equation for continuous chaos, Phys. Lett. 57A (1976), 397–398.

[34] F. Rothe, The periods of the Volterra-Lotka system, J. Reine Angew. Math. 355 (1985), 129–138.

[35] A. Ruiz-Herrera and F. Zanolin, An example of chaotic dynamics in 3D systems via stretching along paths, Ann. Mat. Pura Appl. 193 (2014), 163–185.

[36] A. Ruiz-Herrera and F. Zanolin, Horseshoes in 3D equations with applications to Lotka-Volterra systems, NoDEA Nonlinear Differ. Equ. Appl. 22 (2015), 877–897.

[37] R. Veneziani and S. Mohun, Structural stability and Goodwin's growth cycle, Struct. Change Econ. Dynam. 17 (2006), 437–451.

[38] J. Waldvogel, The period in the Lotka-Volterra system is monotonic, J. Math. Anal. Appl. 114 (1986), 178–184.

[39] W. Zhang, Cyclical economic growth–re-examining the Goodwin model, Acta Math. Appl. Sin. 7 (1991), 114–120.

6 Appendix: Proof of Proposition 2.1

Proof of Proposition 2.1. Given the linked together annuli $\mathcal{C}^{(I)}(\ell_1,\ell_2)$ and $\mathcal{C}^{(II)}(h_1,h_2)$, we call $\mathcal{C}_t^{(I)}(\ell_1,\ell_2)$ (resp. $\mathcal{C}_b^{(I)}(\ell_1,\ell_2)$) the subset of $\mathcal{C}^{(I)}(\ell_1,\ell_2)$ which lies above (resp. below)[10] the horizontal line r, joining $P^{(I)}$ and $P^{(II)}$; analogously, $\mathcal{C}_t^{(II)}(h_1,h_2)$ (resp. $\mathcal{C}_b^{(II)}(h_1,h_2)$) is the subset of $\mathcal{C}^{(II)}(h_1,h_2)$ which lies above (resp. below) r. In this manner it holds that $\mathcal{C}^{(I)}(\ell_1,\ell_2) = \mathcal{C}_t^{(I)}(\ell_1,\ell_2)\cup\mathcal{C}_b^{(I)}(\ell_1,\ell_2)$ and $\mathcal{C}^{(II)}(h_1,h_2) = \mathcal{C}_t^{(II)}(h_1,h_2)\cup\mathcal{C}_b^{(II)}(h_1,h_2)$. Moreover, we introduce the generalized rectangles $\mathcal{A} := \mathcal{C}_t^{(I)}(\ell_1,\ell_2)\cap\mathcal{C}_t^{(II)}(h_1,h_2)$ and $\mathcal{B} := \mathcal{C}_b^{(I)}(\ell_1,\ell_2)\cap\mathcal{C}_b^{(II)}(h_1,h_2)$. Let us fix $m^{(I)}\geq 1$ and $m^{(II)}\geq 1$ such that $m = m^{(I)}m^{(II)} \geq 2$. We are going to show that, if we orientate $\mathcal{A}$ and $\mathcal{B}$ e.g. by setting $\mathcal{A}^- = \mathcal{A}_l^-\cup\mathcal{A}_r^-$ and $\mathcal{B}^- = \mathcal{B}_l^-\cup\mathcal{B}_r^-$, with $\mathcal{A}_l^- := \mathcal{A}\cap\Gamma^{(I)}(\ell_1)$, $\mathcal{A}_r^- := \mathcal{A}\cap\Gamma^{(I)}(\ell_2)$, $\mathcal{B}_l^- := \mathcal{B}\cap\Gamma^{(II)}(h_2)$, $\mathcal{B}_r^- := \mathcal{B}\cap\Gamma^{(II)}(h_1)$, then there exist $m^{(I)}\geq 1$ pairwise disjoint compact subsets $\mathcal{H}_0,\ldots,\mathcal{H}_{m^{(I)}-1}$ of $\mathcal{A}$ such that

$$(\mathcal{H}_i,\Psi^{(I)}) : \widetilde{\mathcal{A}} \overset{\circlearrowleft}{\Longrightarrow} \widetilde{\mathcal{B}}, \quad i=0,\ldots,m^{(I)}-1 \tag{6.1}$$

(cf. Figure 3 (A) for a graphical illustration with $m^{(I)} = 1$), as well as $m^{(II)}\geq 1$ pairwise disjoint compact subsets $\mathcal{K}_0,\ldots,\mathcal{K}_{m^{(II)}-1}$ of $\mathcal{B}$ such that

$$(\mathcal{K}_j,\Psi^{(II)}) : \widetilde{\mathcal{B}} \overset{\circlearrowleft}{\Longrightarrow} \widetilde{\mathcal{A}}, \quad j=0,\ldots,m^{(II)}-1 \tag{6.2}$$

(see Figure 3 (B) for an illustration with $m^{(II)} = 2$). Namely, if this is the case, (C_F) and (C_G) in Theorem 4.1 are fulfilled for the oriented rectangles $\widetilde{\mathcal{A}} := (\mathcal{A},\mathcal{A}^-)$ and $\widetilde{\mathcal{B}} := (\mathcal{B},\mathcal{B}^-)$ with $F = \Psi^{(I)}$ and $G = \Psi^{(II)}$. Since $m = m^{(I)}m^{(II)}\geq 2$, and (C_m) in Theorem 4.1 holds true, too, the Poincaré map $\Psi = \Psi^{(II)}\circ\Psi^{(I)}$ of System (2.4) induces chaotic dynamics on m symbols in $\mathcal{A}$. Recalling that the Poincaré map Ψ is a homeomorphism on $(0,+\infty)^2$, and thus it is injective and continuous in particular on the set $\mathcal{H}^* := \bigcup_{\substack{i=0,\ldots,m^{(I)}-1\\ j=0,\ldots,m^{(II)}-1}} \mathcal{H}_i\cap\left(\Psi^{(I)}\right)^{-1}(\mathcal{K}_j)$, also condition (C_Φ) in Theorem 4.1 is satisfied for $\Phi=\Psi$ and it is then possible to apply Theorem 4.1 to conclude that all the properties listed therein are fulfilled for Ψ.

In view of checking (6.1), we introduce a system of polar coordinates $(\rho^{(I)},\theta^{(I)})$ centered at $P^{(I)}$, so that the solution $\varsigma^{(I)}(t,(u_0,v_0)) = (u(t,(u_0,v_0)),v(t,(u_0,v_0)))$

[10] Namely, t stands for "top" and b stands for "bottom".

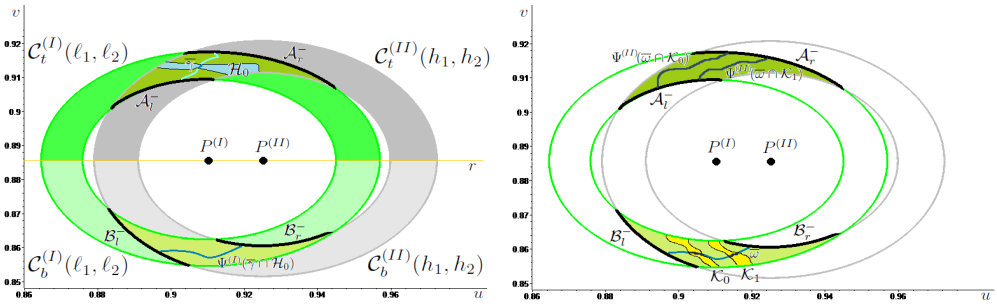

(A) (B)

Figure 3: In (A), given the linked together annuli $\mathcal{C}^{(I)}(\ell_1,\ell_2)$ and $\mathcal{C}^{(II)}(h_1,h_2)$, we draw in orange the straight line r joining the centers $P^{(I)}$, $P^{(II)}$ and separating the top sets $\mathcal{C}_t^{(I)}(\ell_1,\ell_2)$, $\mathcal{C}_t^{(II)}(h_1,h_2)$, colored respectively in green and gray, from the bottom sets $\mathcal{C}_b^{(I)}(\ell_1,\ell_2)$, $\mathcal{C}_b^{(II)}(h_1,h_2)$, colored respectively in light green and light gray. For $\mathcal{A} := \mathcal{C}_t^{(I)}(\ell_1,\ell_2) \cap \mathcal{C}_t^{(II)}(h_1,h_2)$ and $\mathcal{B} := \mathcal{C}_b^{(I)}(\ell_1,\ell_2) \cap \mathcal{C}_b^{(II)}(h_1,h_2)$, suitably oriented by the choice of their left and right sides, we illustrate in (A) the condition (6.1) with $m^{(I)} = 1$ and in (B) the condition (6.2) with $m^{(II)} = 2$.

to System (I) with initial point in $(u_0,v_0) \in (0,+\infty)^2$ can be expressed as $\varsigma^{(I)}(t,(u_0,v_0)) = \|\varsigma^{(I)}(t,(u_0,v_0)) - P^{(I)}\| \, (\cos(\theta^{(I)}(t,(u_0,v_0))), \sin(\theta^{(I)}(t,(u_0,v_0))))$. Moreover, we define the rotation number, describing the normalized angular displacement during the time interval $[0,t] \subseteq [0,T^{(I)}]$ of the solution $\varsigma^{(I)}(t,(u_0,v_0))$ as

$$\mathrm{rot}^{(I)}(t\,,(u_0,v_0)) := \frac{\theta^{(I)}(0,(u_0,v_0)) - \theta^{(I)}(t,(u_0,v_0))}{2\pi} \tag{6.3}$$

in order to count positive the turns around $P^{(I)}$ in the clockwise sense, since orbits for System (I) are run clockwise. Recalling the definition of $\tau^{(I)}(\ell)$, for $\ell > \ell_0^{(I)}$, as a consequence of the star-shapedness with respect to $P^{(I)}$ of the lower contour sets $\{(u,v) \in (0,+\infty)^2 : E^{(I)} \le \ell\}$, with $E^{(I)}$ as in (2.7), we obtain that the following properties

$$\begin{aligned}
\mathrm{rot}^{(I)}(t,(u_0,v_0)) < n &\iff t < n\,\tau^{(I)}(\ell)\\
\mathrm{rot}^{(I)}(t,(u_0,v_0)) = n &\iff t = n\,\tau^{(I)}(\ell)\\
\mathrm{rot}^{(I)}(t,(u_0,v_0)) > n &\iff t > n\,\tau^{(I)}(\ell)
\end{aligned}$$

hold true for every $(u_0, v_0) \in \Gamma^{(I)}(\ell)$, $t \in [0, T^{(I)}]$ and $n \geq 1$. Hence, we have that $\mathrm{rot}^{(I)}(t, (u_0, v_0)) \in (n, n+1) \Longleftrightarrow t \in (n\,\tau^{(I)}(\ell), (n+1)\,\tau^{(I)}(\ell))$.
To check (6.1), let $\gamma : [0,1] \to \mathcal{A}$ be a generic path with $\gamma(0) \in \mathcal{A}_l^-$, $\gamma(1) \in \mathcal{A}_r^-$. For every $\lambda \in [0,1]$, we consider $\Psi^{(I)}(\gamma(\lambda))$, i.e., the position at time $T^{(I)}$ of the solution $\varsigma^{(I)}(t\,, \gamma(\lambda))$ to System (I) starting at $t = 0$ from $\gamma(\lambda) \in \mathcal{A}$, together with the corresponding angular coordinate $\theta^{(I)}(T^{(I)}, \gamma(\lambda))$. We stress that, due to the continuity of γ and by the continuous dependence of the solutions from the initial data, the function $\lambda \mapsto \theta^{(I)}(T^{(I)}, \gamma(\lambda))$ is continuous, too. Moreover, recalling that $\tau^{(I)}(\ell_1) < \tau^{(I)}(\ell_2)$ and $\mathcal{A}_l^- \subset \Gamma^{(I)}(\ell_1)$, $\mathcal{A}_r^- \subset \Gamma^{(I)}(\ell_2)$, we are going to show that if $T^{(I)} > t^{(I)} := \left(m^{(I)} + \frac{7}{2}\right) \frac{\tau^{(I)}(\ell_1)\tau^{(I)}(\ell_2)}{(\tau^{(I)}(\ell_2) - \tau^{(I)}(\ell_1))}$ then $\theta^{(I)}(T^{(I)}, \gamma(1)) - \theta^{(I)}(T^{(I)}, \gamma(0)) > \left(2m^{(I)} + 1\right)\pi$.
If this is true, there exists $n^* \in \mathbb{N}$ such that $[-2(n^*+i)\pi - \pi, -2(n^*+i)\pi]$ is contained in the interval $\{\theta^{(I)}(T^{(I)}, \gamma(\lambda)) : \lambda \in [0,1]\}$ for $i \in \{0, \ldots, m^{(I)} - 1\}$. Thus, by Bolzano theorem, there are $m^{(I)}$pairwise disjoint maximal intervals $[\lambda_i', \lambda_i'']$ of $[0,1]$ such that for $i \in \{0, \ldots, m^{(I)} - 1\}$ it holds that $\{\theta^{(I)}(T^{(I)}, \gamma(\lambda)) : \lambda \in [\lambda_i', \lambda_i'']\} \subseteq [-2(n^*+i)\pi - \pi, -2(n^*+i)\pi]$, with $\theta^{(I)}(T^{(I)}, \gamma(\lambda_i')) = -2(n^*+i)\pi - \pi$ and $\theta^{(I)}(T^{(I)}, \gamma(\lambda_i'')) = -2(n^*+i)\pi$. In order to have the stretching relation (6.1) satisfied, we can then set $\mathcal{H}_i := \{(u_0, v_0) \in \mathcal{A} : \theta^{(I)}(T^{(I)}, (u_0, v_0)) \in [-2(n^*+i)\pi - \pi, -2(n^*+i)\pi]\}$ for $i \in \{0, \ldots, m^{(I)} - 1\}$. Indeed, for $i \in \{0, \ldots, m^{(I)} - 1\}$, $\mathcal{H}_i$ is a compact set containing $\{\gamma(\lambda)) : \lambda \in [\lambda_i', \lambda_i'']\}$. Moreover, for $i \in \{0, \ldots, m^{(I)} - 1\}$ and $\lambda \in [\lambda_i', \lambda_i'']$, it holds that $\gamma(\lambda) \in \mathcal{H}_i$, $\Psi^{(I)}(\gamma(\lambda)) \in \mathcal{C}_b^{(I)}(\ell_1, \ell_2)$ and $E^{(II)}(\Psi^{(II)}(\gamma(\lambda_i'))) \geq h_2$, $E^{(II)}(\Psi^{(II)}(\gamma(\lambda_i''))) \leq h_1$. Hence, there exists an interval $[\lambda_i^*, \lambda_i^{**}] \subseteq [\lambda_i', \lambda_i'']$ such that $\Psi^{(I)}(\gamma(\lambda)) \in \mathcal{B}$ for every $\lambda \in [\lambda_i^*, \lambda_i^{**}]$, and $E^{(II)}(\Psi^{(I)}(\gamma(\lambda_i^*))) = h_2$, $E^{(II)}(\Psi^{(I)}(\gamma(\lambda_i^{**}))) = h_1$. Since $\mathcal{B}_l^- = \mathcal{B} \cap \Gamma^{(II)}(h_2)$, $\mathcal{B}_r^- = \mathcal{B} \cap \Gamma^{(II)}(h_1)$, this means that $\Psi^{(I)}(\gamma(\lambda_i^*)) \in \mathcal{B}_l^-$ and $\Psi^{(I)}(\gamma(\lambda_i^{**})) \in \mathcal{B}_r^-$, concluding the verification of (6.1).
We then have to check that, for any path $\gamma : [0,1] \to \mathcal{A}$ with $\gamma(0) \in \mathcal{A}_l^- = \mathcal{A} \cap \Gamma^{(I)}(\ell_1)$ and $\gamma(1) \in \mathcal{A}_r^- = \mathcal{A} \cap \Gamma^{(I)}(\ell_2)$, if it holds that $T^{(I)} > t^{(I)}$ then $\theta^{(I)}(T^{(I)}, \gamma(1)) - \theta^{(I)}(T^{(I)}, \gamma(0)) > \left(2m^{(I)} + 1\right)\pi$. Since $\mathrm{rot}^{(I)}(t, \gamma(0)) \geq \lfloor t/\tau^{(I)}(\ell_1) \rfloor$ and $\mathrm{rot}^{(I)}(t, \gamma(1)) \leq \lceil t/\tau^{(I)}(\ell_2) \rceil$ for every $t > 0$, it follows that $\mathrm{rot}^{(I)}(t, \gamma(0)) - \mathrm{rot}^{(I)}(t, \gamma(1)) \geq \lfloor t/\tau^{(I)}(\ell_1) \rfloor - \lceil t/\tau^{(I)}(\ell_2) \rceil > t\,\frac{\tau^{(I)}(\ell_2) - \tau^{(I)}(\ell_1)}{\tau^{(I)}(\ell_1)\,\tau^{(I)}(\ell_2)} - 2$ for every $t > 0$. Hence, for $T^{(I)} > t^{(I)}$ it holds that

$$\begin{aligned}\mathrm{rot}^{(I)}(T^{(I)}, \gamma(0)) - \mathrm{rot}^{(I)}(T^{(I)}, \gamma(1)) &> T^{(I)}\,\frac{\tau^{(I)}(\ell_2) - \tau^{(I)}(\ell_1)}{\tau^{(I)}(\ell_1)\,\tau^{(I)}(\ell_2)} - 2 \\ &> m^{(I)} + \tfrac{7}{2} - 2 = m^{(I)} + \tfrac{3}{2} > m^{(I)} + 1.\end{aligned}$$

As a consequence, recalling the definition of $\mathrm{rot}^{(I)}$ given in (6.3), we have that $\theta^{(I)}(T^{(I)},\gamma(1))-\theta^{(I)}(T^{(I)},\gamma(0))>2(m^{(I)}+1)\pi+\theta^{(I)}(0,\gamma(1))-\theta^{(I)}(0,\gamma(0))$. Since $\gamma([0,1])\subset\mathcal{A}:=\mathcal{C}_t^{(I)}(\ell_1,\ell_2)\cap\mathcal{C}_t^{(II)}(h_1,h_2)$, it holds that both $\theta^{(I)}(0,\gamma(0))$ and $\theta^{(I)}(0,\gamma(1))$ belong to $[0,\pi]$, and thus $\theta^{(I)}(0,\gamma(1))-\theta^{(I)}(0,\gamma(0))>-\pi$, from which it follows that $\theta^{(I)}(T^{(I)},\gamma(1))-\theta^{(I)}(T^{(I)},\gamma(0))>(2m^{(I)}+1)\pi$, as needed.

Let us now turn to the proof of the stretching relation in (6.2). Due to its similarity with the verification of (6.1), we will sketch just the main steps. In this case we consider the image through $\Psi^{(II)}$ of any path $\omega:[0,1]\to\mathcal{B}$ joining $\mathcal{B}_l^-$ with $\mathcal{B}_r^-$ and check that it completely crosses $\mathcal{A}$, from $\mathcal{A}_l^-$ to $\mathcal{A}_r^-$, at least $m^{(II)}$ times when $T^{(II)}>t^{(II)}:=\left(m^{(II)}+\frac{7}{2}\right)\frac{\tau^{(II)}(h_1)\tau^{(II)}(h_2)}{(\tau^{(II)}(h_2)-\tau^{(II)}(h_1))}$, recalling that also orbits for System (II) are run clockwise and that $\tau^{(II)}(h_1)<\tau^{(II)}(h_2)$ (see Figure 3 (B) for the case $m^{(II)}=2$). Introducing a system of polar coordinates $(\rho^{(II)},\theta^{(II)})$ centered at $P^{(II)}$, we can define the rotation number as

$$\mathrm{rot}^{(II)}(t\,,(u_0,v_0)):=\frac{\theta^{(II)}(0,(u_0,v_0))-\theta^{(II)}(t,(u_0,v_0))}{2\pi} \tag{6.4}$$

describing the normalized angular displacement during the time interval $[0,t]\subseteq[0,T^{(II)}]$ of the solution $\varsigma^{(II)}(t\,,(u_0,v_0))$ to System (II) with initial point in $(u_0,v_0)\in(0,+\infty)^2$. Like it happened with the proof of (6.1), the key step in the verification of (6.2) consists in showing that if $T^{(II)}>t^{(II)}$ then $\theta^{(II)}(T^{(II)},\omega(1))-\theta^{(II)}(T^{(II)},\omega(0))>\left(2m^{(II)}+1\right)\pi$. Indeed, using Bolzano Theorem, this allows to conclude that there exist $m^{(II)}\geq 1$ pairwise disjoint compact subsets $\mathcal{K}_0,\,\ldots,\,\mathcal{K}_{m^{(II)}-1}$ of $\mathcal{B}$ which satisfy (6.2).

Once that the validity of (6.1) and (6.2) is verified, it follows that $\Psi=\Psi^{(II)}\circ\Psi^{(I)}$ induces chaotic dynamics on m symbols in $\mathcal{A}$ by Theorem 4.1, together with all the properties listed therein.

This concludes the first half of our proof, that will be complete just when we will show that Ψ induces chaotic dynamics on $m=m^{(I)}m^{(II)}\geq 2$ symbols in $\mathcal{B}$, as well. To such aim, we can e.g. orientate $\mathcal{A}$ by setting $\mathcal{A}^{--}=\mathcal{A}_l^{--}\cup\mathcal{A}_r^{--}$, with $\mathcal{A}_l^{--}:=\mathcal{A}\cap\Gamma^{(II)}(h_1)$, $\mathcal{A}_r^{--}:=\mathcal{A}\cap\Gamma^{(II)}(h_2)$, and $\mathcal{B}$ by setting $\mathcal{B}^{--}=\mathcal{B}_l^{--}\cup\mathcal{B}_r^{--}$, with $\mathcal{B}_l^{--}:=\mathcal{B}\cap\Gamma^{(I)}(\ell_1)$, $\mathcal{B}_r^{--}:=\mathcal{B}\cap\Gamma^{(I)}(\ell_2)$, and we verify that the image through $\Psi^{(I)}$ of any path joining in $\mathcal{B}$ the sides $\mathcal{B}_l^{--}$ and $\mathcal{B}_r^{--}$ crosses $\mathcal{A}$, from $\mathcal{A}_l^{--}$ to $\mathcal{A}_r^{--}$, at least $m^{(I)}$ times when $T^{(I)}>t^{(I)}$, and then check that the image through $\Psi^{(II)}$ of any path in $\mathcal{A}$ joining $\mathcal{A}_l^{--}$ with $\mathcal{A}_r^{--}$ crosses $\mathcal{B}$, from $\mathcal{B}_l^{--}$ to $\mathcal{B}_r^{--}$, at least $m^{(II)}$ times when $T^{(II)}>t^{(II)}$. Namely, this amounts to show that there exist $m^{(I)}\geq 1$ pairwise

disjoint compact subsets $\mathcal{H}'_0, \ldots, \mathcal{H}'_{m^{(I)}-1}$ of $\mathcal{B}$ such that

$$(\mathcal{H}'_i, \Psi^{(I)}) : \widetilde{\widetilde{\mathcal{B}}} \pitchfork \widetilde{\widetilde{\mathcal{A}}}, \quad i = 0, \ldots, m^{(I)} - 1, \tag{6.5}$$

as well as $m^{(II)} \geq 1$ pairwise disjoint compact subsets $\mathcal{K}'_0, \ldots, \mathcal{K}'_{m^{(II)}-1}$ of $\mathcal{A}$ such that

$$(\mathcal{K}'_j, \Psi^{(II)}) : \widetilde{\widetilde{\mathcal{A}}} \pitchfork \widetilde{\widetilde{\mathcal{B}}}, \quad j = 0, \ldots, m^{(II)} - 1, \tag{6.6}$$

where we set $\widetilde{\widetilde{\mathcal{B}}} := (\mathcal{B}, \mathcal{B}^{--})$ and $\widetilde{\widetilde{\mathcal{A}}} := (\mathcal{A}, \mathcal{A}^{--})$ (see Figure 4). In such case, (C_F) and (C_G) in Theorem 4.1 are fulfilled for the newly introduced oriented rectangles $\widetilde{\widetilde{\mathcal{B}}} := (\mathcal{B}, \mathcal{B}^{--})$, $\widetilde{\widetilde{\mathcal{A}}} := (\mathcal{A}, \mathcal{A}^{--})$ and with $F = \Psi^{(I)}$, $G = \Psi^{(II)}$. Since $m = m^{(I)} m^{(II)} \geq 2$, it is then possible to apply Theorem 4.1 to conclude that the Poincaré map $\Psi = \Psi^{(II)} \circ \Psi^{(I)}$ of System (2.4) induces chaotic dynamics on m symbols in $\mathcal{B}$, as well. Moreover, Ψ has all the features listed in Theorem 4.1 because (C_Φ) therein holds true, too, as $\Phi = \Psi$ is injective and continuous in particular on the set $\mathcal{H}'^{*} := \bigcup_{\substack{i = 0, \ldots, m^{(I)} - 1 \\ j = 0, \ldots, m^{(II)} - 1}} \mathcal{H}'_i \cap \left(\Psi^{(I)}\right)^{-1} (\mathcal{K}'_j)$.
Due to their resemblance to (6.1) and (6.2), we leave to the reader the details in the verification of (6.5) and (6.6), that allow to complete the proof.

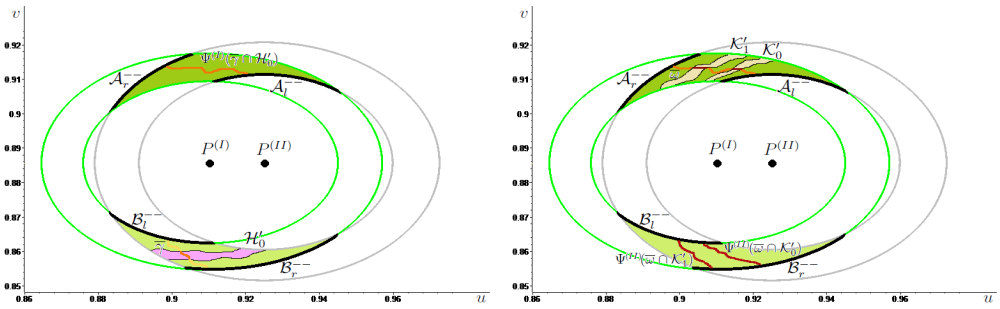

(A) (B)

Figure 4: For the sets $\mathcal{A}$ and $\mathcal{B}$ introduced in Figure 3, which we now orientate in a different manner by suitably choosing the left and the right sides, we illustrate in (A) the stretching relation (6.5) with $m^{(I)} = 1$ and in (B) the condition (6.6) with $m^{(II)} = 2$.

Focusing on the first half of the proof of Proposition 2.1, in which we show that Ψ induces chaotic dynamics in $\mathcal{A}$, in Figure 3 (A) we provide a qualitative representation of what happens when the stretching relation in (6.1) is

fulfilled with $m^{(I)} = 1$ and in Figure 3 (B) we illustrate the condition (6.2) with $m^{(II)} = 2$. To have (6.1) satisfied with $m^{(I)} = 1$ we need to verify that the image through $\Psi^{(I)}$ of any path γ (in cyan) joining in $\mathcal{A}$ its left and right sides crosses $\mathcal{B}$ once from left to right when $T^{(I)}$ is sufficiently large. This is true in Figure 3 (A) since, calling $\mathcal{H}_0$ the compact subset of $\mathcal{A}$ in pale blue and setting $\overline{\gamma} := \gamma([0,1])$, it holds that $\overline{\gamma} \cap \mathcal{H}_0$ (in blue) is transformed by $\Psi^{(I)}$ into a path (in blue) connecting $\mathcal{B}_l^-$ and $\mathcal{B}_r^-$ in $\mathcal{B}$. To check (6.2) with $m^{(II)} = 2$ we need to verify that the image through $\Psi^{(II)}$ of any path ω (in blue) joining in $\mathcal{B}$ its left and right sides crosses $\mathcal{A}$ twice from left to right when $T^{(II)}$ is large enough. This is true in Figure 3 (B) due to the existence of the pairwise disjoint compact subsets $\mathcal{K}_0\,, \mathcal{K}_1$ of $\mathcal{B}$ (in yellow) with the property that $\Psi^{(II)}(\overline{\omega} \cap \mathcal{K}_i)$ (in dark blue) connects $\mathcal{A}_l^-$ and $\mathcal{A}_r^-$ in $\mathcal{A}$, for $i \in \{1, 2\}$.
Similarly, in regard to the second half of the proof of Proposition 2.1, in which we show that Ψ induces chaotic dynamics in $\mathcal{B}$, we illustrate in Figure 4 (A) condition (6.5) with $m^{(I)} = 1$ and in Figure 4 (B) condition (6.6) with $m^{(II)} = 2$. Notice that $\mathcal{A}$ and $\mathcal{B}$ need now to be oriented in a different manner with respect to Figure 3 to have the stretching relations in (6.5) and (6.6) satisfied. Indeed, in Figure 4 (A) we draw (in lilac) the compact subset $\mathcal{H}_0'$ of $\mathcal{B}$ with the property that the restriction to it (represented in orange) of any path γ (in light orange) joining $\mathcal{B}_l^{--}$ and $\mathcal{B}_r^{--}$ in $\mathcal{B}$ is transformed by $\Psi^{(I)}$ into a path (in orange) connecting $\mathcal{A}_l^{--}$ and $\mathcal{A}_r^{--}$ in $\mathcal{A}$. In (B) we draw (in beige) the two disjoint compact subsets $\mathcal{K}_0'$, $\mathcal{K}_1'$ of $\mathcal{A}$ such that the restriction to them (represented in dark orange) of any path ω (in orange) joining $\mathcal{A}_l^{--}$ and $\mathcal{A}_r^{--}$ in $\mathcal{A}$ is transformed by $\Psi^{(II)}$ into paths (in dark orange) connecting $\mathcal{B}_l^{--}$ and $\mathcal{B}_r^{--}$ in $\mathcal{B}$.